

# Nonylphenol and Cetyl Alcohol Polyethoxylates Disrupt Thyroid Hormone Receptor Signaling to Disrupt Metabolic Health

Roxanne Bérubé,<sup>1</sup> Brooklynn Murray,<sup>1</sup> Thomas A. Kocarek,<sup>1</sup> Katherine Gurdziel,<sup>1,2</sup> and Christopher D. Kassotis<sup>1</sup> 

<sup>1</sup>Institute of Environmental Health Sciences and Department of Pharmacology, Wayne State University, Detroit, MI 48202, USA

<sup>2</sup>Genome Sciences Core, Wayne State University, Detroit, MI 48202, USA

**Correspondence:** Christopher D. Kassotis, PhD, Institute of Environmental Health Sciences and Department of Pharmacology, School of Medicine, Wayne State University, 2111 Integrative Biosciences Center, 6135 Woodward Ave, Detroit, MI 48236, USA. Email: [christopher.kassotis@wayne.edu](mailto:christopher.kassotis@wayne.edu).

## Abstract

Surfactants are molecules with both hydrophobic and hydrophilic structural groups that adsorb at the air-water or oil-water interface and serve to decrease the surface tension. Surfactants combine to form micelles that surround and break down or remove oils, making them ideal for detergents and cleaners. Two of the most important classes of nonionic surfactants are alkylphenol ethoxylates (APEOs) and alcohol ethoxylates (AEOs). APEOs and AEOs are high production-volume chemicals that are used for many industrial and residential purposes, including laundry detergents, hard-surface cleaners, paints, and pesticide adjuvants. Commensurate with better appreciation of the toxicity of APEOs and the base alkylphenols, use of AEOs has increased, and both sets of compounds are now ubiquitous environmental contaminants. We recently demonstrated that diverse APEOs and AEOs induce triglyceride accumulation and/or preadipocyte proliferation in vitro. Both sets of contaminants have also been demonstrated as obesogenic and metabolism-disrupting in a developmental exposure zebrafish model. While these metabolic health effects are consistent across models and species, the mechanisms underlying these effects are less clear. This study sought to evaluate causal mechanisms through reporter gene assays, relative binding affinity assays, coexposure experiments, and use of both human cell and zebrafish models. We report that antagonism of thyroid hormone receptor signaling appears to mediate at least a portion of the polyethoxylate-induced metabolic health effects. These results suggest further evaluation is needed, given the ubiquitous environmental presence of these thyroid-disrupting contaminants and reproducible effects in human cell models and vertebrate animals.

**Key Words:** endocrine-disrupting chemicals, adipogenesis, alcohol ethoxylates, ethoxylated surfactants, mixtures, alkylphenol ethoxylates

**Abbreviations:** AEO, alcohol ethoxylate; APEO, alkylphenol ethoxylate; AR, androgen receptor; CetAEO, cetyl alcohol ethoxylate; DMSO, dimethyl sulfoxide; ER, estrogen receptor; FBS, fetal bovine serum; GR, glucocorticoid receptor; hMSCs, human mesenchymal stem cells; LXR $\alpha$ , liver X receptor alpha; MEHP, mono-2-ethylhexyl phthalate; NPEO, nonylphenol ethoxylate; PPAR $\gamma$ , peroxisome proliferator-activated receptor gamma; ppm, parts per million; RNA-seq, RNA sequencing; RXR $\alpha$ , retinoid X receptor alpha; T3, triiodothyronine; TR $\beta$ , thyroid hormone receptor beta.

Surfactants are molecules with both hydrophobic and hydrophilic structural groups that adsorb at the air-water or oil-water interface and serve to decrease the surface tension. Surfactants combine to form micelles that surround and break down or remove oils, making them ideal for detergents and cleaners. Two of the most important classes of nonionic surfactants are alkylphenol ethoxylates (APEOs) and alcohol ethoxylates (AEOs). APEOs are high production-volume chemicals that are used for many industrial and residential purposes, including laundry detergents, hard-surface cleaners, paints, and pesticide adjuvants (1-4). Nonylphenol ethoxylates (NPEOs; a class of APEOs) comprise approximately 80% of the total annual production of nonionic surfactants (5). Ethoxylates degrade into base alkylphenols (eg, nonylphenol, octylphenol), highly lipophilic chemicals with demonstrated toxicity (6-8). AEOs are high production-volume chemicals designed as safer alternatives to APEOs, and are also used in detergents, cleaners, and cosmetics (9). Commensurate with better appreciation of the toxicity of

APEOs, use of AEOs has increased, and both sets of compounds are ubiquitous environmental contaminants (5, 9-18).

Our laboratory and others have demonstrated APEOs and AEOs in indoor house dust (19), municipal wastewater, surface, ground, and finished drinking water (16, 20), and in unconventional oil and gas wastewater (12), indicating widespread human exposure. Because of the toxicity of base alkylphenols and efficient (90%-95%) polyethoxylate chain-shortening during wastewater treatment (21-23), there has been movement away from the APEOs for toxicity concerns. Degradation and removal of APEOs/AEOs are dependent on temperature, oxygen content, and adsorption, which can contribute to lower degradation and greater subsequent releases into receiving streams (23-25). As such,  $\mu\text{g/L}$  concentrations of APEOs have been reported in wastewater/effluent, surface and groundwater, while  $\text{ng/L}$  concentrations have been reported in drinking water (5, 9-18). A recent meta-analysis suggests these concentrations are consistent in water sources over time (26). Our laboratory

reported ng/L- $\mu$ g/L concentrations of AEOs ( $C_6$ - $C_{10}$  alkyl chain length and 2-12 ethoxymethyl chain number) in unconventional oil and gas flowback water and treated effluent (11-13), as well as at a high frequency of detection in indoor house dust (19). The US Environmental Protection Agency estimates that children consume 60 to 100 mg of indoor house dust each day via routine hand-to-mouth behavior (27), supporting the potential for bioaccumulation (9, 28-31). Human exposure to the base compounds has been shown in 90% to 100% of human urine, breast milk, and other human biospecimens (32-34), and exposure to the polyethoxylates is also consistently reported in humans (9, 34-38). Indeed, despite analytical challenges in the measurement of specific chain-length APEOs and AEOs, due to a lack of commercially available specific ethoxylate chain length standards, they are routinely found in household dust and other environmental matrices (5, 9-18, 26, 36, 39-41) at concentrations orders of magnitude exceeding those of compounds such as flame retardants, plasticizers, and per/polyfluoroalkyl substances (PFAS) that have considerably greater perceived toxicity. However, there is a relatively little toxicity and health effect data on APEOs and AEOs.

Our laboratory has recently published several assessments of polyethoxylate-induced metabolic health toxicity (40, 42-44). Using a well-established in vitro model of adipogenesis, we demonstrated that diverse APEOs and AEOs induce triglyceride accumulation and/or preadipocyte proliferation (40, 42-44). Specifically, APEOs and AEOs in a range of carbon chain lengths ( $C_{11}$ - $C_{16}$  alkyl chain lengths) induced up to 250% triglyceride accumulation (marker for adipocyte differentiation, relative to rosiglitazone-induced maximum) and up to 150% increased DNA content (preadipocyte proliferation, relative to differentiated vehicle control) in the 3T3-L1 murine preadipocyte model. These adipogenic effects appeared to be mediated both by the presence and the length of the ethoxylate chains, as the respective base compounds exhibited minimal activity (42). These effects were reproducible across in vitro models, with consistent patterns of response observed between 3T3-L1 murine preadipocytes and both male and female human mesenchymal stem cells (hMSCs) (43, 44). Similarly, both APEOs and AEOs induced obesogenic effects in a developmental exposure zebrafish model (43, 44). We have focused this project on representative APEOs and AEOs that are the most reported in environmental matrices (8, 9, 12, 14, 26, 36, 40, 45): NPEOs and cetyl AEOs (CetAEOs).

The goals of this study were to assess the causal mechanisms underlying the metabolism-disrupting effects of NPEOs and CetAEOs. A range of polyethoxylate chain length NPEOs and CetAEOs were examined for molecular mechanisms underlying their adipogenic and obesogenic effects using a combination of receptor reporter gene assays, relative binding affinity assays, and coexposure experiments in hMSCs.

## Materials and Methods

### Chemicals

Stock solutions of high-purity chemicals were prepared in 100% dimethyl sulfoxide (DMSO) (Sigma catalog No. D2650), using the molecular weight (control chemicals) or average molecular weight (ethoxylated surfactants). Since none of the ethoxylates included here have commercially available pure standards, we used commercial mixtures with average ethoxylate chain

lengths. Chemicals used are described in Table 1. All stock and working solution vials were stored at  $-20^{\circ}\text{C}$  between uses.

### Reporter Gene Activity Bioassays

Human embryonic kidney cells (HEK-293T/17; ATCC No. CRL-11268, lot No. 70022180) were maintained in growth medium (Dulbecco's Modified Eagle Medium [DMEM]-HG, Gibco No. 11995, with 10% fetal bovine serum (FBS), Sigma F2442-500ML, 100 U/mL penicillin and 100- $\mu$ g/mL streptomycin, Gibco 15140). Human endometrial adenocarcinoma cells (Ishikawa; Sigma No. 99040201, lot No. 17C011) were maintained in growth medium (MEM, Gibco 11090, with 5% newborn calf serum, Fisher 16010159, 1% GlutaMAX, Gibco 35050, 1% nonessential amino acids, Gibco 11140, 100-U/mL penicillin and 100- $\mu$ g/mL streptomycin). Human hepatocellular carcinoma cells (HepG2; ATCC No. HB-8065, lot No. 70032516) cells were maintained in DMEM-HG with 10% FBS, 100 U/mL penicillin and 100- $\mu$ g/mL streptomycin. Zebrafish embryonic fibroblast cells (ZF4; ATCC No. CRL-2050, lot No. 63991780) were maintained in DMEM:F12 (Gibco No. 11320) with 10% FBS, 100-U/mL penicillin, and 100- $\mu$ g/mL streptomycin. All cells were maintained in a subconfluent state in 5%  $\text{CO}_2$ -supplemented incubators, with human cell lines at  $37^{\circ}\text{C}$  and zebrafish cells at  $28^{\circ}\text{C}$ . To prepare for transfection, near confluent flasks were switched to white assay medium (same base media without phenol red, and with charcoal-stripped FBS) at least 2 days prior to transfection. After 2 days, flasks were treated with a combination of Lipofectamine LTX & Plus reagent (Invitrogen catalog No. 15338-100) and plasmids in Opti-MEM (Gibco 11058), then recovered overnight in white assay media. Plasmids consisted of human hormone receptor constructs: peroxisome proliferator-activated receptor gamma (PPAR $\gamma$ : pcDNA-PPAR $\gamma$ 1), thyroid hormone receptor beta (TR $\beta$ : hTR $\beta$ 1-pSG5), glucocorticoid receptor (GR: pRST7-GR), retinoid X receptor alpha (RXR $\alpha$ : pcDNA-RXR $\alpha$ ), liver X receptor alpha (LXR: pcDNA-LXR $\alpha$ ), and androgen receptor (AR: CMV-AR1). An estrogen receptor alpha (ER $\alpha$ ) expression plasmid was not used due to high endogenous receptor expression in Ishikawa cells. Reporter gene plasmids were used as follows: PPAR $\gamma$ : DR1-luciferase, TR $\beta$ : pGL4-TK-2X-TADR4, GR: MMTV-luciferase, RXR $\alpha$ : DR1-luciferase, LXR: DR1-luciferase, AR: PSA Enhancer-luciferase, and ER $\alpha$ : 3xERE-TK-luciferase. These plasmids were generous gifts of the Donald McDonnell Lab (Duke University) other than AR plasmids, which were gifts of the Dennis Lubahn Lab (University of Missouri). A constitutively active NanoLuc luciferase normalization plasmid (Promega catalog No. N1501) was used for normalization to putative cytotoxicity. PPAR $\gamma$ , RXR $\alpha$ , and TR $\beta$  plasmids were transfected into HEK293 cells; AR into HepG2 cells; and GR and ER into Ishikawa cells.

Zebrafish receptor plasmids (PPAR $\gamma$ , TR $\beta$ , GR, RXR $\alpha$ , LXR $\alpha$  and AR) were created via Thermo GeneArt service, inserting the sequence of the zebrafish receptor ligand binding domains into the pcDNA3.4-TOPO backbone. The plasmid DNA was purified from transformed bacteria and concentration was determined by UV spectroscopy. Constructs were verified by sequencing, and plasmids were amplified to 1 mg and shipped to the laboratory for direct use in assays. Transfections were performed as described earlier but with the zebrafish receptors, human receptor response elements, normalization vector, and ZF4 cell line, with all assays in zebrafish cells performed at  $28^{\circ}\text{C}$ .

**Table 1. Polyethoxylates and control chemicals**

Chemical	Acronym	CAS no.	Manufacturer	Catalog no.	Avg MW	Molecular formula
Alkylphenols/ethoxylates						
4-Nonylphenol	NPEO(0)	84852-15-3	Acros Organics	416240010	220.4	C <sub>15</sub> H <sub>24</sub> O
Nonylphenol ethoxylate (1-2)	NPEO(1-2)	N/A	Chem Service	S-346	294	C <sub>15</sub> H <sub>24</sub> O(C <sub>2</sub> H <sub>5</sub> O) <sub>1-2</sub>
Nonylphenol ethoxylate (4)	NPEO(4)	N/A	Chem Service	S-347	396	C <sub>15</sub> H <sub>24</sub> O(C <sub>2</sub> H <sub>5</sub> O) <sub>4</sub>
Nonylphenol ethoxylate (6)	NPEO(6)	N/A	Chem Service	S-348	484	C <sub>15</sub> H <sub>24</sub> O(C <sub>2</sub> H <sub>5</sub> O) <sub>6</sub>
Nonylphenol ethoxylate (9-10)	NPEO(9-10)	N/A	Chem Service	S-350	602.8	C <sub>15</sub> H <sub>24</sub> O(C <sub>2</sub> H <sub>5</sub> O) <sub>9-10</sub>
Nonylphenol ethoxylate (20)	NPEO(20)	N/A	Chem Service	S-354	1101	C <sub>15</sub> H <sub>24</sub> O(C <sub>2</sub> H <sub>5</sub> O) <sub>20</sub>
Alcohols/ethoxylates						
Cetyl alcohol	CetAEO(0)	36653-82-4	Chem Service	N-11416-1G	242.5	C <sub>16</sub> H <sub>33</sub> OH
Cetyl alcohol ethoxylate (1-2)	CetAEO(2)	N/A	Sigma	388831-100G	330	C <sub>16</sub> H <sub>33</sub> (OCH <sub>2</sub> CH <sub>2</sub> ) <sub>2</sub> OH
Cetyl alcohol ethoxylate (4)	CetAEO(4)	N/A	Parchem	Ceteth-4	419	C <sub>16</sub> H <sub>33</sub> (OCH <sub>2</sub> CH <sub>2</sub> ) <sub>4</sub> OH
Cetyl alcohol ethoxylate (6)	CetAEO(6)	N/A	Barnet	BC-5.5	507	C <sub>16</sub> H <sub>33</sub> (OCH <sub>2</sub> CH <sub>2</sub> ) <sub>6</sub> OH
Cetyl alcohol ethoxylate (10)	CetAEO(10)	N/A	Barnet	BC-10	683	C <sub>16</sub> H <sub>33</sub> (OCH <sub>2</sub> CH <sub>2</sub> ) <sub>10</sub> OH
Cetyl alcohol ethoxylate (20)	CetAEO(20)	N/A	Chem Service	NG-S317-1G	1123	C <sub>16</sub> H <sub>33</sub> (OCH <sub>2</sub> CH <sub>2</sub> ) <sub>20</sub> OH
Control chemicals						
Tributyltin chloride	TBT	1461-22-9	Sigma	442869	325.5	[CH <sub>3</sub> (CH <sub>2</sub> ) <sub>3</sub> ] <sub>3</sub> SnCl
Mono(2-ethylhexyl) phthalate	MEHP	4376-20-9	Santa Cruz Biotechnology	sc-396467	278.3	C <sub>16</sub> H <sub>22</sub> O <sub>4</sub>
Rosiglitazone	ROSI	122320-73-4	Sigma	R2408-10mg	357.43	C <sub>18</sub> H <sub>19</sub> N <sub>3</sub> O <sub>3</sub> S
Dexamethasone	DEX	50-02-2	Sigma	D4902-25mg	392.46	C <sub>22</sub> H <sub>29</sub> FO <sub>5</sub>
LG100268	—	153559-76-3	Sigma	SML0279-5mg	363.49	C <sub>24</sub> H <sub>29</sub> NO <sub>2</sub>
T0901317	—	293754-55-9	Sigma	T2320-10mg	481.33	C <sub>17</sub> H <sub>12</sub> NSO <sub>3</sub> F <sub>9</sub>
Flutamide	—	13311-84-7	Sigma	F9397-5G	276.21	C <sub>11</sub> H <sub>11</sub> F <sub>3</sub> N <sub>2</sub> O <sub>3</sub>
BMS-564,929	BMS	627530-84-1	Tocris	5274	305.72	C <sub>14</sub> H <sub>12</sub> ClN <sub>3</sub> O <sub>3</sub>
1-850	—	251310-57-3	Sigma	609315-M	463.41	C <sub>21</sub> H <sub>20</sub> F <sub>3</sub> N <sub>5</sub> O <sub>4</sub>
Triiodothyronine	T3	6893-02-3	Sigma	T2877-100mg	650.97	C <sub>15</sub> H <sub>12</sub> I <sub>3</sub> NO <sub>4</sub>
17β-estradiol	E2	50-28-2	Sigma	E8875-250mg	272.38	C <sub>18</sub> H <sub>24</sub> O <sub>2</sub>
Fulvestrant	—	129453-61-8	Sigma	I4409-25MG	606.77	C <sub>32</sub> H <sub>47</sub> F <sub>5</sub> O <sub>3</sub> S
T0070907	—	313516-66-4	Sigma	T8703-5MG	277.66	C <sub>12</sub> H <sub>8</sub> ClN <sub>3</sub> O <sub>3</sub>
Dimethyl sulfoxide	DMSO	67-68-5	Sigma	34869-100mL	78.1	(CH <sub>3</sub> ) <sub>2</sub> SO

Chemical identification, ordering information, and basic physicochemical properties for each of the alkylphenols, alcohols, polyethoxylates, and control chemicals examined in this study. Molecular formulae contain base carbon number as well as average ethoxylate chain number. Abbreviations: MW, molecular weight; N/A, not available.

Transfected cells were subsequently seeded at 50 000 to 70 000 cells per well into 96-well tissue culture plates and allowed to settle. Settled cells were then induced with doses spanning 4 to 6 orders of magnitude of test chemicals using a 0.1% DMSO vehicle. Cells were treated for 18 to 22 hours and then lysed for dual luciferase assays (Promega, PR-E1960). Raw luminescence values were converted to fold inductions relative to the vehicle control responses and were then used to calculate percentage bioactivities. For agonist bioassays, polyethoxylate-induced responses were compared to the maximal positive control-induced responses to determine percentage activities. For antagonist bioassays, cells were treated with a half-maximal response concentration of a positive control chemical (as determined in agonist bioassays) in the absence or presence of different concentrations of polyethoxylates, and activities were calculated as percent enhancement or suppression relative to the positive control-induced response. These concentrations, determined based on full-dose response curves of positive control chemicals, were 1-nM T3 for TR antagonism testing, 1 pM for ER antagonism testing, and 1-nM BMS-564 929 for AR antagonism testing. Statistically significant reduction in constitutively

active NanoLuc luciferase activity (>15%) was used as an indirect marker of toxicity and receptor bioactivities were reported only in the absence of apparent toxicity. Control transfections were performed with the luciferase promoter backbones in the absence of the hormone response elements; no significant induction of luminescence was observed for any test chemicals in the absence of the hormone response elements.

### Relative Binding Affinity Assays

Relative binding affinity assays for ERα were performed using commercially available assays (Thermo-Fisher PolarScreen No. A15884) according to the manufacturer's instructions (46). Relative binding affinity assays for TRβ were performed using Thermo-Fisher components and purified full-length human TRβ. Briefly, fluorescent rhodamine-labeled triiodothyronine (T3) was synthesized using a previously described reaction by the Duke University Small Molecule Core (47). In brief, T3 was mixed with equimolar TRITC (10 mM of each; Sigma cat No. 87918) to conjugate rhodamine to the amino group of the T3. The reaction was stirred and allowed

to proceed overnight. Products were purified by column chromatography and checked by mass spectrometry to ensure more than 95% purity. Solvent was then evaporated, leaving behind purified rhodamine conjugated T3 as a free-flowing burgundy powder and stored at  $-20^{\circ}\text{C}$ . While functionality was not assessed prior to use, the previous publications directly assessed functionality using this conjugation protocol (47, 48). We prepared a stock solution at 10 mM in DMSO and stored at  $-20^{\circ}\text{C}$  until use. Relative binding affinity experiments used Thermo Red Screening Buffer, with purified TR $\beta$  and fluorescent T3 as per the Thermo-Fisher PolarScreen Universal Protocol (49). A saturating concentration of T3 (20  $\mu\text{M}$ ) was added to minimum control wells, then various doses of test compounds were added at 2 $\times$  concentrations in 384-well plates. Then the TR $\beta$  protein was combined with the rhodamine-labeled T3 and added to all wells except for the no receptor control wells. These received only rhodamine-labeled T3 and the Red Screening Buffer, along with the maximum polarization control wells. The assay plate was mixed and incubated, protected from light, for 2 hours, then the fluorescence polarization was measured (535/590 nm, bandwidths of 25/20 nm) and half-maximal inhibitory concentration (IC<sub>50</sub>) values were determined based on changes in fluorescence polarization and comparison to maximum, minimum, and no receptor control wells. The K<sub>d</sub> for T3 displacement from the fluorescent T3-bound TR $\beta$  was approximately 25 nM, which confirmed similar performance to previous assessments using this labeled T3 (47, 48).

### Coactivator Recruitment Assays

LanthaScreen TR-FRET nuclear receptor coactivator recruitment assays were performed according to the manufacturer's instructions (Fisher Sci catalog No. PV4686) (50). Briefly, no agonist and maximal agonist controls were prepared in TR-FRET coregulator buffer with maximal agonist control set at 1  $\mu\text{M}$  T3. Dilution series of all test chemicals and T3 control were then prepared using 12-point dose response curves from 10  $\mu\text{M}$  to 16.9 pM, then diluted with 0.5-nM TR $\beta$  ligand-binding domain and also fluorescein-SRC2-2 (200 nM) combined with Tb anti-GST antibody (2 nM). Plates were mixed and incubated at room temperature, protected from light, for 2 hours. Plates were then read at wavelengths of 520 and 495 nm and percent activity was calculated using emission ratios as follows: (emission ratio of compound – emission ratio of no agonist control) / (emission ratio of no agonist control – emission ratio of max agonist control)  $\times$  100%. Assays are not validated in antagonism mode by the manufacturer and so only agonism mode was performed.

### Coexposure Experiments in Human Mesenchymal Stem Cells

Adipogenic responses to NPEOs and CetAEOs have been previously published in 3T3-L1 cells (42) and human mesenchymal stem cells (hMSCs) (43, 44). To further assess causal mechanisms underlying these effects, we performed coexposure experiments with known receptor ligands to determine their abilities to reverse polyethoxylate-induced effects. To assess potential causal effects through PPAR $\gamma$ , we performed coexposures with 10- $\mu\text{M}$  T0070907. For AR, we performed coexposures with 10- $\mu\text{M}$  BMS-564 929, for TR $\beta$ , we performed coexposures with 10- $\mu\text{M}$  T3 and also 10-nM T3,

and for ER, we performed coexposures with 10-nM 17 $\beta$ -estradiol or 10-nM fulvestrant (agonist and antagonist, respectively).

Adipogenesis differentiation assays were performed as described in detail previously (43, 44, 51, 52). In short, Zenbio hMSCs (catalog No. HBMMS-C-F, lot No. HBMMS-C0 71819A, female, White, aged 35 years) were maintained in a subconfluent state in basal medium (DMEM/Nutrient Mixture F-12, DMEM/F-12; Gibco No. 11320, with 10% FBS, 100-U/mL penicillin and 100- $\mu\text{g}/\text{mL}$  streptomycin) and were used for all assays between passage 8 (on receipt) and 13 (no more than 5 passages from receipt). Human MSCs were seeded into 96-well plate plates at approximately 10 000 cells/well and induced to differentiate according to a unified protocol (43, 44, 51). After settling for at least 1 day, medium was replaced with test chemicals with or without coexposures diluted in differentiation medium as described earlier (Zenbio catalog No. DM-2; contains DMEM/Ham's F-12, HEPES, FBS, biotin, pantothenate, human insulin, dexamethasone, 3-isobutyl-1-methylxanthine [IBMX], a proprietary PPAR $\gamma$  agonist, penicillin, streptomycin, amphotericin B). After 3 days, differentiation medium was replaced with fresh test chemical dilutions in adipocyte maintenance medium (AMM; Zenbio catalog No. AM-1). AMM-diluted test chemicals were refreshed every 3 to 5 days until assay at day 21. Triglyceride accumulation and DNA content were measured 21 days after the start of differentiation as described previously (53-57). Cells were rinsed with Dulbecco's phosphate-buffered saline (DPBS, Gibco 14040). Dye mixture at 200  $\mu\text{L}$  was then added to all wells (19-mL DPBS; 20 drops NucBlue reagent, Thermo catalog No. R37605; and 500  $\mu\text{L}$  of 40  $\mu\text{g}/\text{mL}$  Nile Red solution, Sigma catalog No. 72485-100MG). Plates were then incubated, protected from light, for approximately 40 minutes at room temperature, then fluorescence was measured (485 nm/572 nm excitation/emission for Nile Red and 360/460 for NucBlue). Fold change relative to the vehicle control response (0.1% DMSO) was calculated and then triglyceride accumulation determined as percent activity relative to the maximum rosiglitazone-induced response. DNA content was calculated as percentage change from the vehicle control response, and this was then used to normalize triglyceride accumulation. Three biological replicates (separate assays and cell passages), each including 4 technical replicates (intraplate replicates), were performed for all adipogenesis assays.

### Transcriptomic Assessment of Human Mesenchymal Stem Cells

hMSCs were cultured in basal media and isolated using TRIzol prior to induction of commitment and differentiation. RNA isolation and expression analysis was accomplished at the Wayne State University Genome Sciences Core with the following methods. RNA was isolated using Zymo's Direct-zol RNA Purification Kit following the standard protocol. An aliquot of the RNA was assessed by microfluidics using the ScreenTape for the Agilent 2200 TapeStation. The electrophoretogram, RNA integrity number (RIN), and the ratio of the 28S:18S RNA bands were collectively examined to determine overall quality of the RNA. RNA sequencing (RNA-seq) was used to determine expression profiles. Lexogen's QuantSeq 3'mRNA-seq Library Prep Kit (FWD for Illumina) was used for building RNA-seq libraries using 100 ng of total RNA in 5  $\mu\text{L}$  of nuclease-free ultrapure water. Libraries were quantified on the Qubit and Agilent 2200 TapeStation using the DNA

High Sensitivity Screen tape. The barcoded libraries were multiplexed at equimolar concentrations and sequenced (75 bp reads; >5 M reads per sample) on the NovaSeq 6000. Data was demultiplexed using Illumina's CASAVA 1.8.2 software. After quality was assessed (58), reads were aligned to the human genome (Build mm10) (59) and tabulated for each gene region (60). Differential gene expression analysis was used to compare transcriptome changes between conditions (61). Significantly altered genes (log fold change  $\geq 2$ ; false discovery rate  $\leq 0.05$ ) were used to identify affected pathways (62). The data generated have been deposited in NCBI's Gene Expression Omnibus (63) and are accessible through GEO Series accession number GSE280008.

### Statistical Analysis

Cell data are presented as means  $\pm$  SEM from 4 technical replicates of 3 independent biological replicates. Kruskal-Wallis with Dunn's multiple comparisons test was performed to determine statistically significant differences across concentrations and relative to DMSO controls ( $P < .05$  considered statistically significant), as well as between zebrafish and human receptor bioactivities. Statistical comparisons were made using GraphPad Prism 10.0.

## Results

Alkylphenol and alcohol polyethoxylates were assessed for potential endocrine mechanisms underlying previously described adipogenic responses in vitro and proobesogenic responses in vivo via receptor reporter gene assays, relative binding affinity assays, and coexposure experiments to assess causation.

### Peroxisome Proliferator Activated Receptor Gamma Activity

We previously published a lack of polyethoxylate-mediated PPAR $\gamma$  activation via stable-transfected reporter gene assays and coactivator recruitment assays (42). In this study, we used a transient transfection reporter gene assay in human cells with human PPAR $\gamma$ . We again describe no significant activity for any of the polyethoxylates on human PPAR $\gamma$  (Fig. 1A and 1B). However, we report robust activation of the zebrafish PPAR $\gamma$ , with every alkylphenol and ethoxylate activating zebrafish PPAR $\gamma$  ranging from 65% relative to the mono-2-ethylhexyl phthalate (MEHP) control up to 173% agonism for the NPEO-6 medium chain length ethoxylate (Fig. 1C). Considerably lower activity was observed for the cetyl alcohol polyethoxylates, with CetAEO-6 inducing 23% agonism relative to the maximal MEHP response and CetAEO-4 and -20 inducing 16% to 17% agonism (Fig. 1D).

### Glucocorticoid Receptor Activity

We next assessed activation of the GR as another primary adipogenic pathway (56, 64, 65). Again, we noted no statistically significant activation of the human GR above the baseline response for either the alkylphenol or alcohol polyethoxylates (Fig. 2A and 2B). However, polyethoxylates did activate zebrafish GR, with responses ranging from 32% of the dexamethasone-induced maximum for the base nonylphenol to 57% for NPEO-2, a lower efficacy but greater potency response for NPEO-4 (48%), and no significant activity for NPEO-6, -10, or -20 (Fig. 2C). A similar pattern of responses was observed for the CetAEOs, with agonism

for the lower ethoxylate compounds only. Cetyl alcohol induced 39% agonism relative to the dexamethasone-induced maximum, CetAEO-2 induced the highest activity (63%), and CetAEO-4 and -6 induced significant but lower responses (52% and 28%, respectively). Neither CetAEO-10 nor -20 induced any significant activation of zebrafish GR (Fig. 2D). The maximal responses for nonylphenol, NPEO-2, -4, cetyl alcohol, CetAEO-2, -4, and -6 were all significantly greater than the agonist responses observed for hGR.

### Retinoid X Receptor Activity

Polyethoxylates were next tested for activation of RXR $\alpha$ . None of the NPEOs activated RXR $\alpha$ , though the base nonylphenol exhibited 38% of the maximal LG100268-induced response (Fig. 3A). No significant activity was observed for any of the CetAEOs on human RXR $\alpha$  (Fig. 3B). Again, in contrast to human receptor responses, the longer-chain length NPEOs induced significant agonism for zebrafish RXR $\alpha$ , with NPEO-6, -10, and -20 inducing 18% to 25% agonism relative to the maximal LG100268-induced response (Fig. 3C). Medium and long CetAEOs also activated zebrafish RXR $\alpha$ , with CetAEO-4 and -6 inducing 20% and 37% agonism relative to the positive control maximum, respectively, and CetAEO-20 inducing a more potent and efficacious response (45%; Fig. 3D). While RXR $\alpha$  agonism was significantly greater for nonylphenol with human RXR $\alpha$ , zebrafish RXR $\alpha$  exhibited significantly greater agonist bioactivities for NPEO-6, -10, -20, CetAEO-2, -4, -6, and -20.

### Liver X Receptor Activity

None of the polyethoxylates were able to activate human LXR $\alpha$  (Fig. 4A and 4B). In contrast, low activity was observed for zebrafish LXR $\alpha$ . NPEO-20 induced 37% activation relative to the T0901317-induced maximum response and NPEO-2 induced a 100-fold less potent response of 16% agonism relative to the positive control (Fig. 4C). Cetyl alcohol polyethoxylates (-4, -10, and -20) promoted 20% to 23% agonism relative to the positive control maximum (Fig. 4D). The longest chain NPEOs (-10 and -20) as well as cetyl alcohol and CetAEO-4, -10, and -20 had significantly greater maximal LXR $\alpha$  agonism for the zebrafish receptor than the human receptor.

### Androgen Receptor Antagonism

Antagonism of AR is another well-described adipogenic mechanism (56, 64, 65). Nonylphenol polyethoxylates were able to significantly antagonize the half-maximal BMS-564 929 activation of human AR. Specifically, NPEO-6 induced 28% receptor antagonism, NPEO-10 induced 43% receptor antagonism, and NPEO-20 induced 65% receptor antagonism (Fig. 5A). Cetyl alcohol polyethoxylates were also able to antagonize AR action. These effects were primarily focused in the longer-chain length polyethoxylates, with CetAEO-6, -10, and -20 exhibiting 65% to 71% antagonism of the half-maximal BMS-564 929 response (Fig. 5B). Similar responses were observed for the zebrafish AR, with longer-chain length polyethoxylates inducing significant AR antagonism; NPEO-6, -10, and -20 induced 28%, 43%, and 65% antagonism of the half-maximal BMS-564 929 response, respectively (Fig. 5C). Each of the CetAEOs induced significant AR antagonism, though similarly to human AR, the longer-chain length CetAEOs induced the greatest degree of

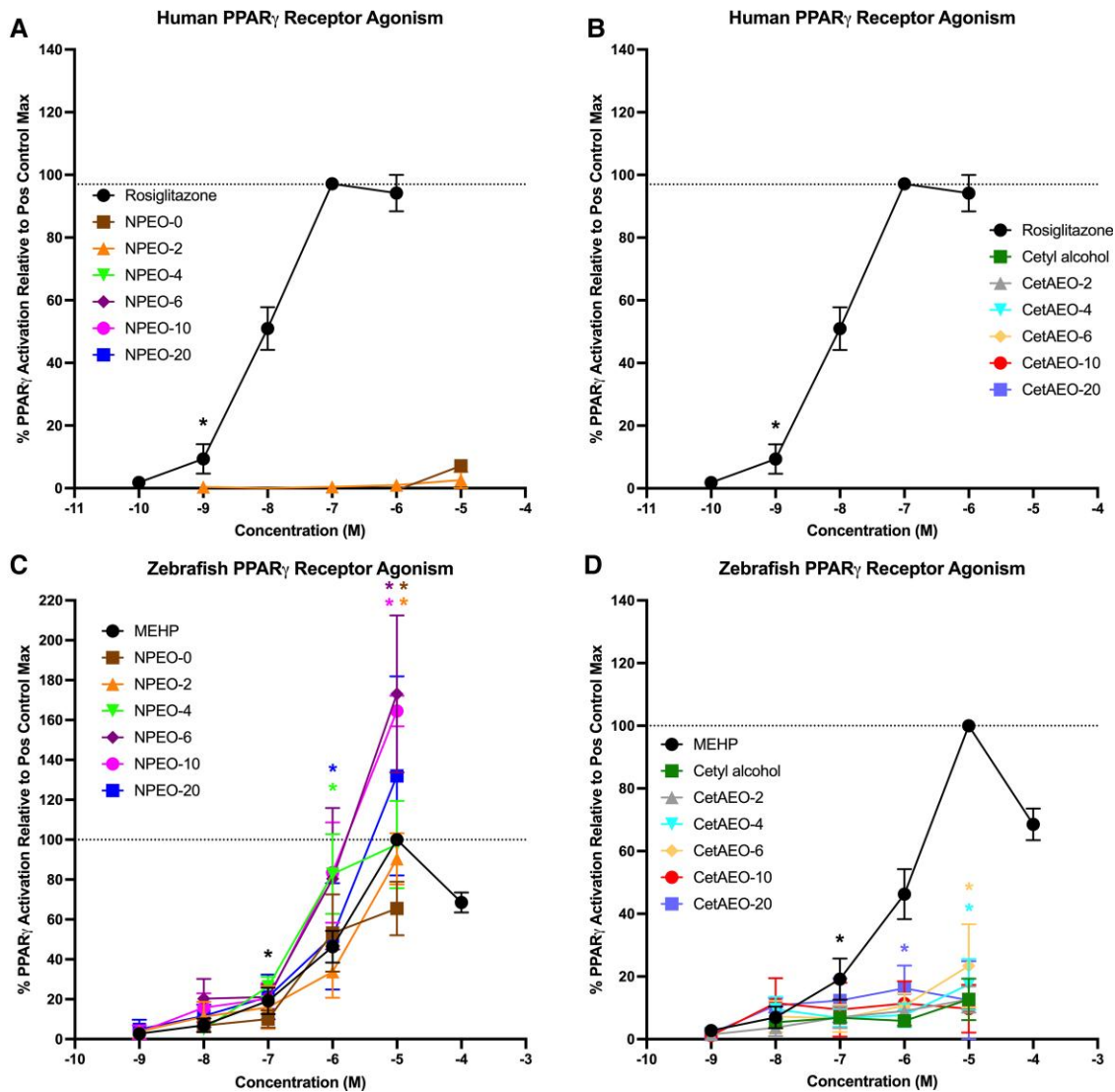


**Figure 1.** Peroxisome proliferator-activated receptor gamma bioactivities. Each polyethoxylate was tested for disruption of both human and zebrafish peroxisome proliferator receptor gamma (PPAR $\gamma$ ). Human PPAR $\gamma$  agonism was measured relative to rosiglitazone-induced maximum for A, nonylphenol polyethoxylates and for B, cetyl alcohol polyethoxylates. Zebrafish PPAR $\gamma$  agonism was measured relative to mono(2-ethylhexyl) phthalate (MEHP)-induced maximum for C, nonylphenol polyethoxylates and for D, cetyl alcohol polyethoxylates. Data presented as mean  $\pm$  SEM from 3 independent experiments. \*Lowest concentration with statistically significant increase over vehicle control response; *P* less than .05, as per Kruskal-Wallis in GraphPad Prism 10. Dotted line represents mean positive control maximum response, and may not always reflect exactly 100% due to differences in maximal concentration between assays.

antagonism. CetAEO-6, -10, and -20 induced 31%, 39%, and 22% antagonism of half-maximal BMS-564 929 response, respectively, though shorter chain length polyethoxylates and the base cetyl alcohol hydrophobe also induced significant antagonism (Fig. 5D). While some significant differences existed between species, these were less pronounced than the previously described agonist bioactivities for other receptors. Short-chain nonylphenols (nonylphenol, NPEO-2, NPEO-4) and CetAEO-4 exhibited greater antagonism for the zebrafish AR, whereas CetAEO-6, -10, and -20 exhibited stronger maximal AR antagonism for human AR.

### Thyroid Hormone Receptor Antagonism

Antagonism of TR $\beta$  was assessed next as a previously described robust adipogenic pathway (56, 64, 65). The longer-chain length NPEOs significantly antagonized the half-maximal T3

activation of human TR $\beta$ . Specifically, NPEO-6, -10, and -20 induced TR $\beta$  antagonism ranging from 49% to 73%, with the greatest effects observed for the longest-chain length polyethoxylates (Fig. 6A). Each of the CetAEOs as well as the base alcohol induced significant TR $\beta$  antagonism. This was lowest for the base alcohol and the low-chain length (-2, -4) polyethoxylates, with antagonism ranging from 17% to 27% reduction of the half-maximal T3 response. The longer-chain length ethoxylates (-6, -10, and -20) induced a greater degree of antagonism, ranging from 47% to 62% (Fig. 6B). Responses on zebrafish TR $\beta$  were more varied. Only the nonethoxylated and low ethoxylate chain length NPEOs induced significant antagonism of zebrafish TR $\beta$ , with antagonism ranging from 29% to 71% inhibition of half-maximal T3 response (Fig. 6C). In contrast to the NPEOs, the CetAEOs induced similar effects on zebrafish TR $\beta$  as for human. The longer-chain length polyethoxylates induced significant antagonism ranging from 39% to 57% of half-

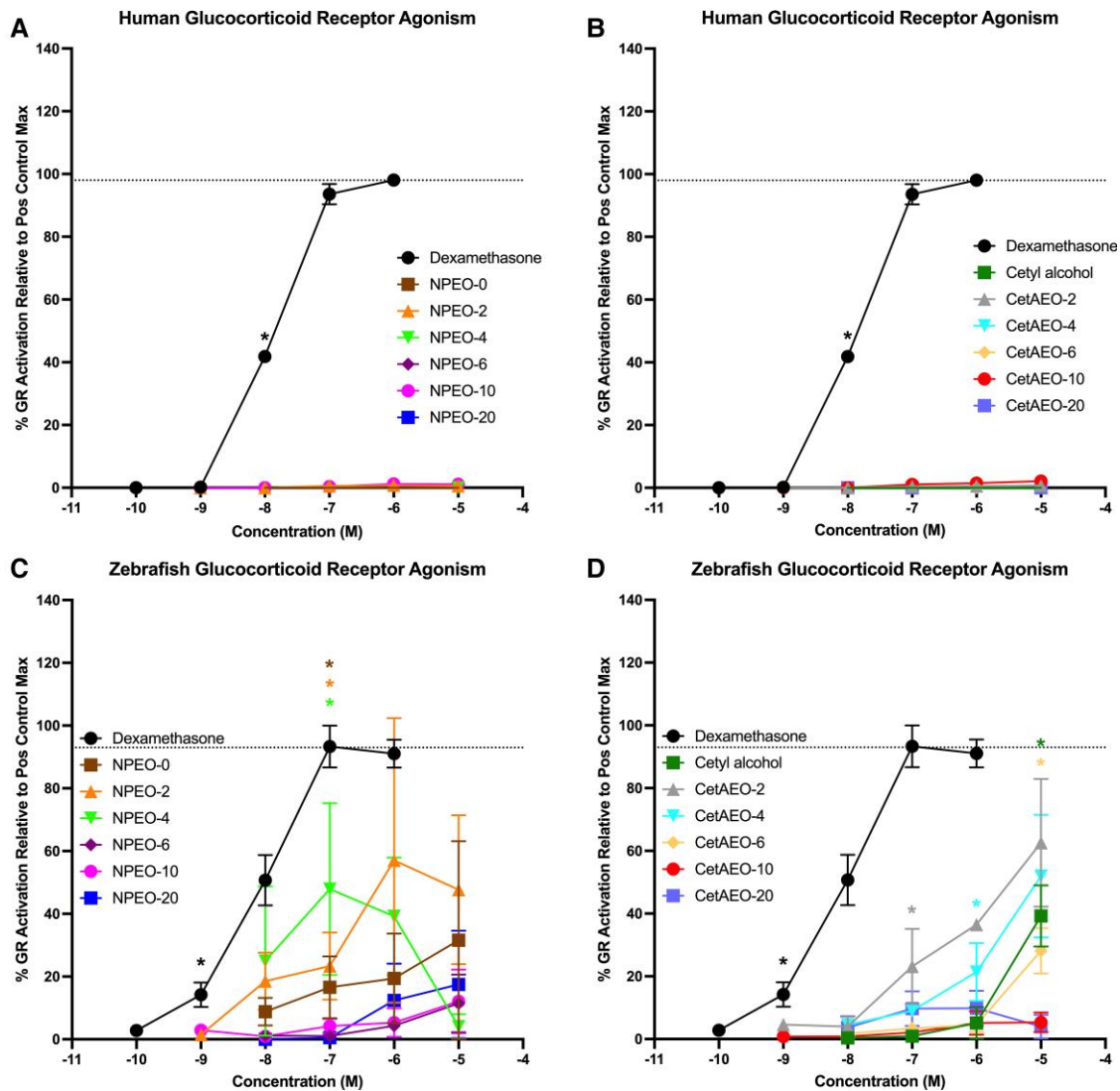


**Figure 2.** Glucocorticoid receptor (GR) bioactivities. Each polyethoxylate was tested for disruption of both human and zebrafish GR. Human GR agonism was measured relative to dexamethasone-induced maximum for A, nonylphenol polyethoxylates and for B, cetyl alcohol polyethoxylates. Zebrafish GR agonism was measured relative to dexamethasone-induced maximum for C, nonylphenol polyethoxylates and for D, cetyl alcohol polyethoxylates. Data presented as mean  $\pm$  SEM from 3 independent experiments. \*Lowest concentration with statistically significant increase over vehicle control response; *P* less than .05, as per Kruskal-Wallis in GraphPad Prism 10. Dotted line represents mean positive control maximum response, and may not always reflect exactly 100% due to differences in maximal concentration between assays.

maximal T3 response (Fig. 6D). To determine if these antagonistic effects were occurring directly at the level of the receptor or through indirect interactions, relative binding affinity assays were used with the human TR $\beta$ . Neither the NPEOs nor the CetAEOs were able to significantly displace fluorescently labeled T3 from TR $\beta$ , suggesting that polyethoxylate-mediated antagonism of TR $\beta$  bioactivation occurred indirectly (Fig. 6E and 6F). Again, these effects were relatively similar across species, with no differences observed for the CetAEOs. Some differences were observed for the NPEOs, where nonylphenol and NPEO-4 had significantly greater maximal TR $\beta$  antagonism for zebrafish TR $\beta$  and NPEO-6, -10, and -20 had significantly greater maximal TR $\beta$  antagonism for human TR $\beta$ . Further assessment was performed to assess the relative ability of the polyethoxylates to recruit SRC2-2 and act as agonists of ligand-dependent coactivator recruitment. Interestingly, every cetyl alcohol and CetAEO was able to robustly recruit SRC2-2 (percentage activation >50%), with significant activation at

low to moderate nM concentrations (Fig. 6H). In contrast, while greater than 40% significant activation was observed for nonylphenol and NPEO-20 and for other NPEOs at lower efficacies, these effects were also considerably less potent, occurring at  $\mu$ M concentrations (Fig. 6G).

### Estrogen Receptor Disruption

ER disruption has been reported for the base nonylphenol and some of the NPEOs; previous reports suggested that increasing polyethoxylate chain length decreased ER agonism, yet the data suggest there may be intermediate chain-length effects that could increase ER agonism (66). To examine this, we assessed disruption of human ER $\alpha$ . As previously described, the base nonylphenol exerted robust ER agonism up to 101% relative to the maximal estradiol-induced response; however, with a potency that was several orders of magnitude lower. NPEO-2 induced an even more efficacious response of up to

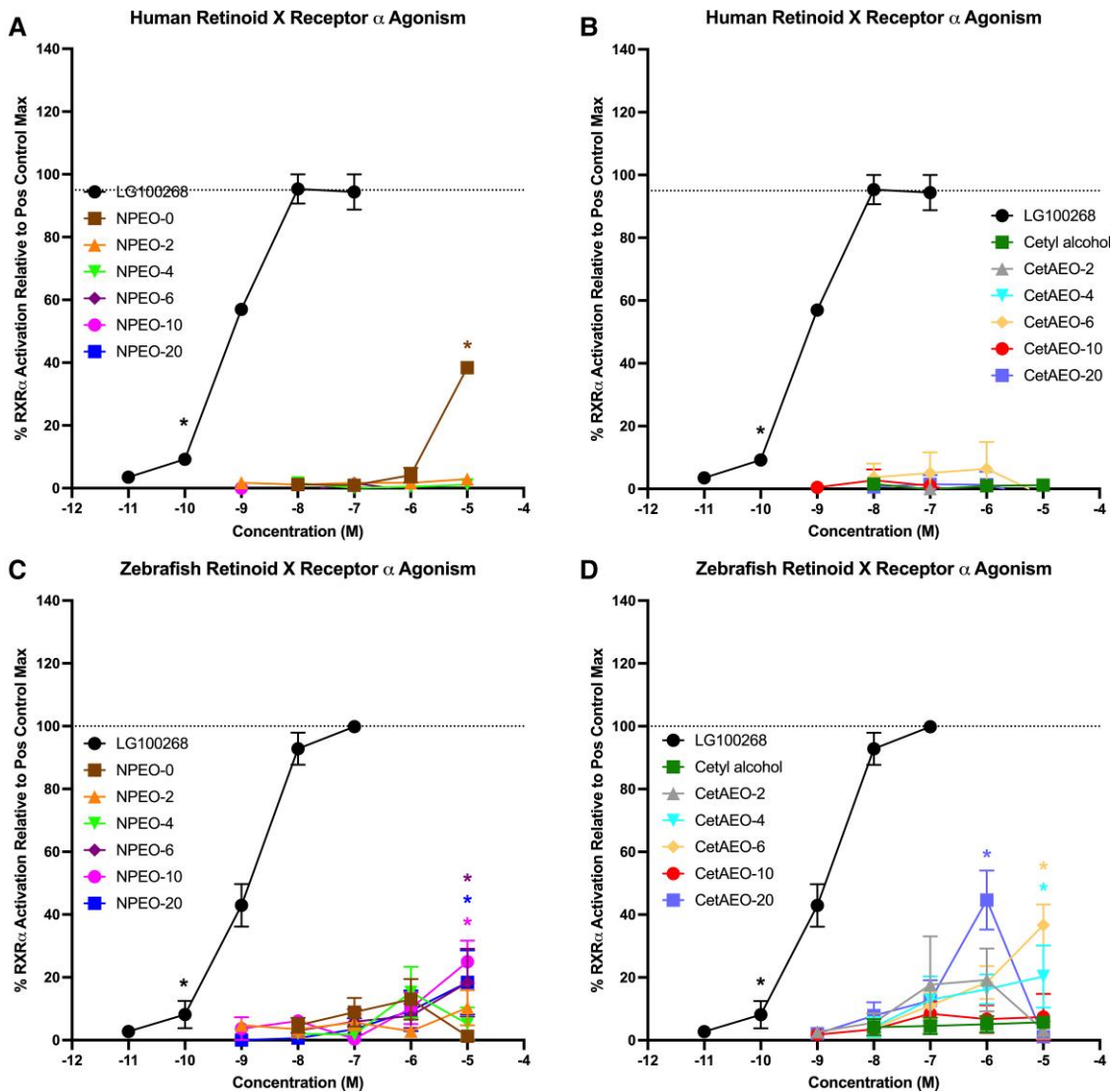


**Figure 3.** Retinoid X receptor alpha (RXR $\alpha$ ) bioactivities. Each polyethoxylate was tested for disruption of both human and zebrafish RXR $\alpha$ . Human RXR $\alpha$  agonism was measured relative to LG100268-induced maximum for A, nonylphenol polyethoxylates and for B, cetyl alcohol polyethoxylates. Zebrafish RXR $\alpha$  agonism was measured relative to LG100268-induced maximum for C, nonylphenol polyethoxylates and for D, cetyl alcohol polyethoxylates. Data presented as mean  $\pm$  SEM from 3 independent experiments. \*Lowest concentration with statistically significant increase over vehicle control response; *P* less than .05, as per Kruskal-Wallis in GraphPad Prism 10. Dotted line represents mean positive control maximum response, and may not always reflect exactly 100% due to differences in maximal concentration between assays.

113% agonism. Decreased agonism was seen with increasing polyethoxylate chain length (eg, NPEO-4 induced 51% agonism; Fig. 7A). The CetAEOs induced limited ER agonism, with the base cetyl alcohol exhibiting 13% agonism relative to the maximal estradiol response and CetAEO-2 exhibiting a robust 84% agonist response. None of the higher ethoxylate chain length CetAEOs induced significant ER agonism (Fig. 7B). We next examined ER antagonism, finding that the longer-chain length NPEOs, which exhibited the least agonism, exhibited minimal ER antagonism relative to the half-maximal estradiol-induced response. Specifically, NPEO-10 and -20 induced 24% and 33% antagonism (Fig. 7C). Interestingly, the CetAEOs demonstrated more robust ER antagonism. While the base compound exhibited no significant ER antagonism, CetAEO-2 and -4 exhibited 20% to 25% antagonism of the half-maximal estradiol response and CetAEO-6, -10, and -20 induced increasing levels of antagonism from 54% to 81% (Fig. 7D). Relative binding affinity assays were then performed with human ER $\alpha$  to determine

direct vs indirect effects. The base nonylphenol and the medium to long chain NPEOs significantly displaced fluorescent estradiol from ER $\alpha$ , supporting direct effects at the level of the receptor (Fig. 7E). Similarly, the longer-chain length CetAEOs displaced fluorescent estradiol, whereas the base and shorter-chain length CetAEOs did not significantly displace the fluorescent ligand (Fig. 7F).

### Effects of Coexposures With Known Receptor Ligands on Polyethoxylate-induced Adipogenesis

We have observed consistent adipogenic effects both in murine and human adipogenesis models (42-44) as well as obesogenic effects in zebrafish (43, 44). Therefore, we settled on further assessment of 3 molecular mechanisms most likely to be causal factors in these effects. While effects on PPAR $\gamma$  differed between human and zebrafish receptors, PPAR $\gamma$  is a critically important pathway for adipogenesis, so this was selected as one pathway for assessment. Coexposures were performed in hMSCs with

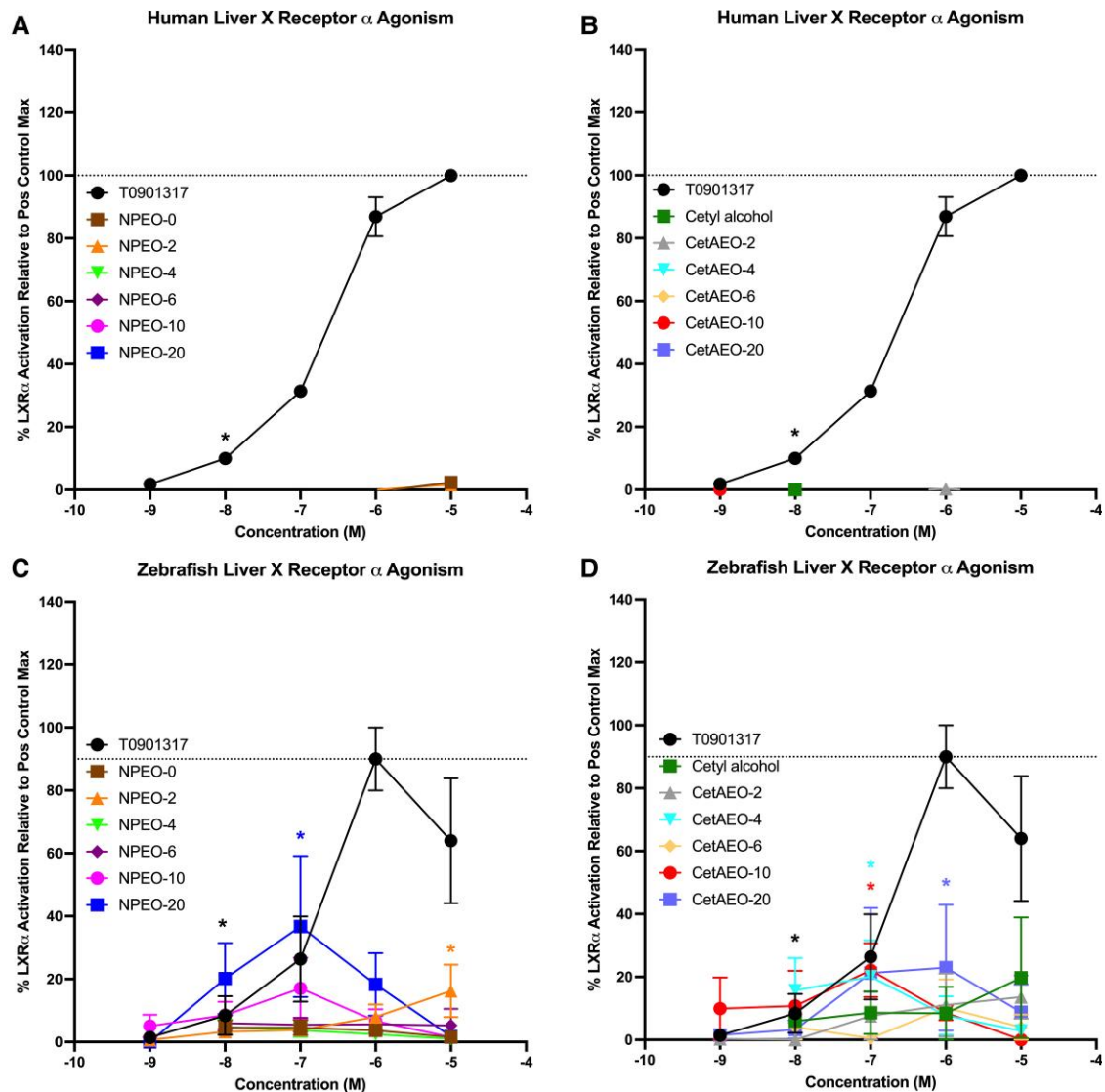


**Figure 4.** Liver X receptor alpha (LXR $\alpha$ ) bioactivities. Each polyethoxylate was tested for disruption of both human and zebrafish LXR $\alpha$ . Human LXR $\alpha$  agonism was measured relative to T0901317-induced maximum for A, nonylphenol polyethoxylates and for B, cetyl alcohol polyethoxylates. Zebrafish LXR $\alpha$  agonism was measured relative to T0901317-induced maximum for C, nonylphenol polyethoxylates and for D, cetyl alcohol polyethoxylates. Data presented as mean  $\pm$  SEM from 3 independent experiments. \*Lowest concentration with statistically significant increase over vehicle control response; *P* less than .05, as per Kruskal-Wallis in GraphPad Prism 10. Dotted line represents mean positive control maximum response, and may not always reflect exactly 100% due to differences in maximal concentration between assays.

polyethoxylates and 10- $\mu$ M T0070907. Coexposures significantly decreased polyethoxylate-induced triglyceride accumulation for every examined polyethoxylate, suggesting a causal or contributory role in the adipogenic effects (Fig. 8A). However, these effects were observed to be indirect, with T0070907 able to attenuate adipogenesis promoted through diverse mechanisms, including GR, TR, and AR (Fig. 9), whereas other control chemicals did not significantly affect adipogenesis operating through pathways other than their own. AR antagonism was next assessed, as patterns of antagonistic response between human and zebrafish AR were comparable. Coexposure experiments with polyethoxylates and 10- $\mu$ M BMS-564 929 resulted in no significant reduction of triglyceride accumulation for any of the tested polyethoxylates, although CetAEO-4 significantly increased AR activation, suggesting some interaction between the AR agonist and polyethoxylates (Fig. 8B). Lastly, antagonism was observed consistently across human and zebrafish

TR $\beta$  for at least the medium and long polyethoxylate compounds, so recovery with T3 was examined using both low and high concentrations. T3 coexposure of 10  $\mu$ M significantly reduced polyethoxylate-induced triglyceride accumulation for every NPEO (not the base nonylphenol) as well as the base cetyl alcohol and CetAEOs-2, -4, and -6 (the longest-chain length CetAEOs did not appreciably change; Fig. 8C). Using a 10-nM T3 coexposure, none of the NPEOs had any significant change in triglyceride accumulation, whereas recovery was still observed for the CetAEOs, with significant decreases observed for CetAEO-2 and -4, and near-significant reductions for cetyl alcohol, CetAEO-6, -10, and -20 (*P* < .10; Fig. 8D). Recovery was also evaluated using both an ER agonist and antagonist. The 10-nM 17 $\beta$ -estradiol coexposure increased the triglyceride accumulation for the longer-chain length NPEOs (-6, -10, and -20), without appreciably changing any other polyethoxylates (Fig. 8E). In contrast, 10-nM fulvestrant significantly inhibited

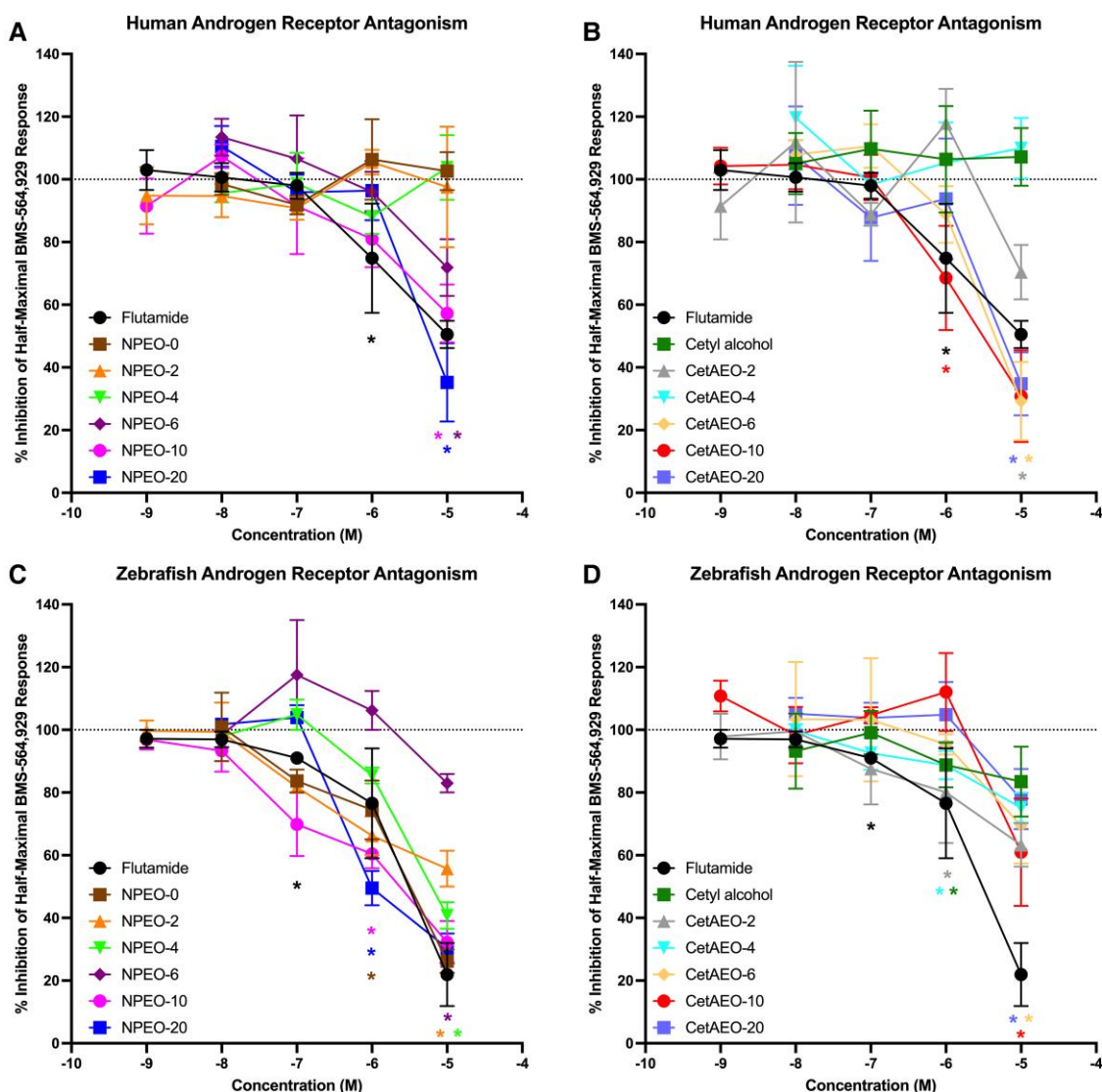


**Figure 5.** Androgen receptor (AR) antagonist bioactivities. Each polyethoxylate was tested for antagonism of both human and zebrafish AR. Significant antagonism of human AR (significant decrease in half-maximal BMS-564 929-induced response) was measured for A, nonylphenol polyethoxylates and for B, cetyl alcohol polyethoxylates. Significant antagonism of zebrafish AR (significant decrease in half-maximal BMS-564 929-induced response) was measured for C, nonylphenol polyethoxylates and for D, cetyl alcohol polyethoxylates. Data presented as mean  $\pm$  SEM from 3 independent experiments. \*Lowest concentration with statistically significant decrease from half-maximal positive control-induced response; *P* less than .05, as per Kruskal-Wallis in GraphPad Prism 10. Dotted line represents half-maximal added agonist response for antagonism or binding affinity assays; decrease from baseline reflects antagonism or displacement of agonist from receptor and increase represents additive agonism response.

polyethoxylate-induced triglyceride accumulation for nonylphenol, NPEO-2, -4, cetyl alcohol, and CetAEO-4, while it appeared to exacerbate the effects for the longer-chain length NPEOs (Fig. 8F). These experiments support a contributory role of TR $\beta$  antagonism in the polyethoxylate-induced adipogenic effects.

## Discussion

We have previously described an adipogenic and obesogenic role both of NPEOs and CetAEOs in murine preadipocytes, hMSCs, and developmentally exposed zebrafish (42-44). This work aimed to determine a putative causal or contributory mechanism in the observed metabolic health effects. As such, we were looking for bioactivities that were shared between human and zebrafish models, especially for the medium-chain length polyethoxylates that seemed to exhibit the greatest magnitude effects both in vitro and in vivo. To

that end, paired receptor reporter gene assays were performed in human and zebrafish cells and with human and zebrafish receptors to assess interspecies comparisons (Fig. 10).

We focused on 6 endocrine pathways that we and others have shown have clear metabolic health effects and pathways shown to promote adipogenesis in vitro (64, 65, 67, 68). Four of these receptors had relatively disparate responses between human and zebrafish receptor bioactivities, including PPAR $\gamma$ , RXR $\alpha$ , LXR $\alpha$ , and GR. For each of these receptors, human responses were significantly lower for each of the polyethoxylates as compared to the zebrafish receptors. None of the base compounds had any agonist activity for these human receptors except nonylphenol for RXR $\alpha$ . PPAR $\gamma$  has been well characterized in humans, with 2 different reporter gene assays demonstrating no activity and both relative binding affinity and coactivator recruitment experiments exhibiting no interaction of these polyethoxylates with human PPAR $\gamma$  (42). In contrast, robust agonism was observed for zebrafish PPAR $\gamma$ , particularly for the NPEOs.

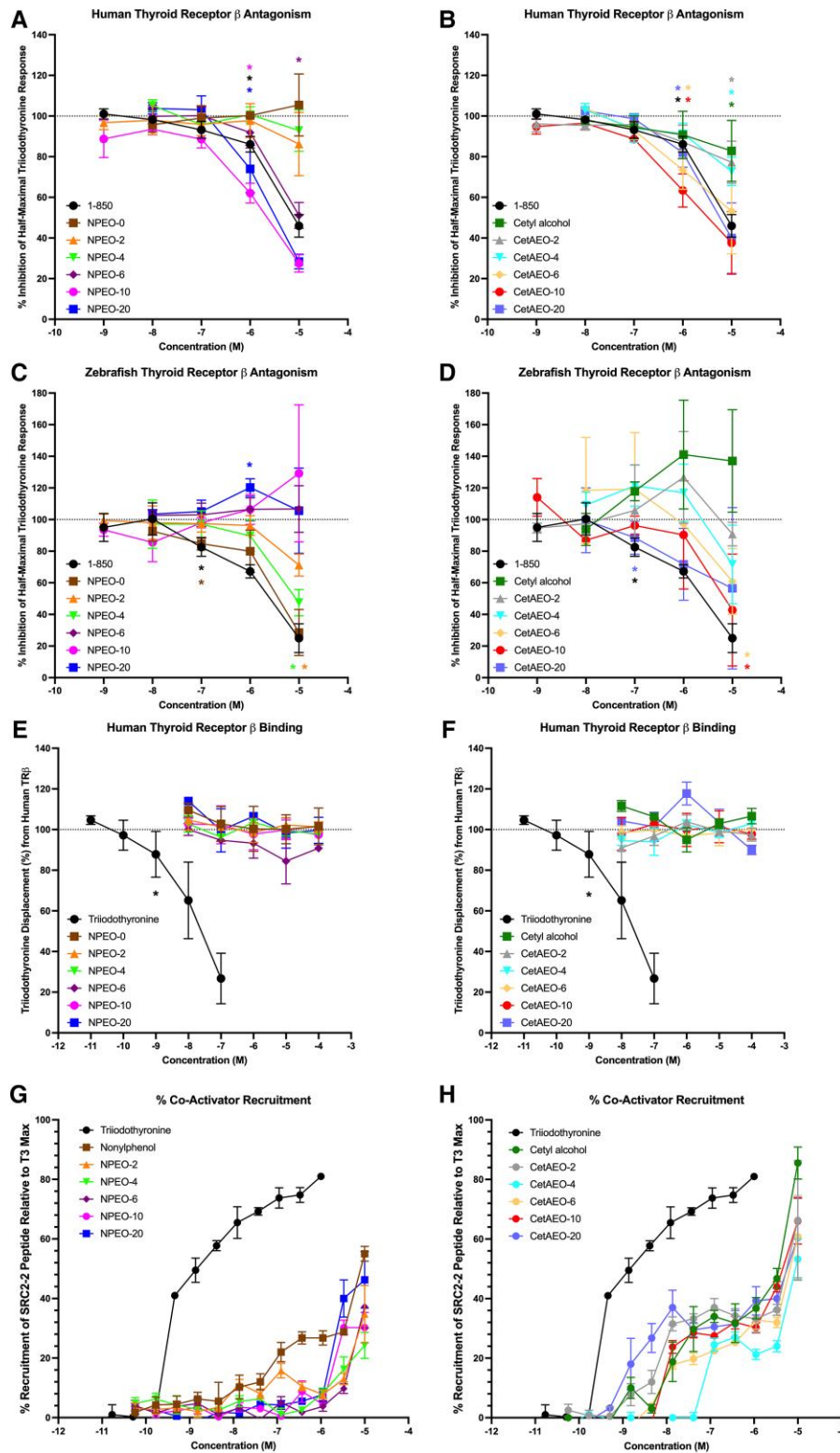


**Figure 6.** Thyroid receptor beta antagonist bioactivities. Each polyethoxylate was tested for antagonism of both human and zebrafish thyroid hormone receptor beta (TR $\beta$ ). Significant antagonism of human TR $\beta$  (significant decrease in half-maximal triiodothyronine-induced response) was measured for A, nonylphenol polyethoxylates and for B, cetyl alcohol polyethoxylates. Significant antagonism of zebrafish TR $\beta$  (significant decrease in half-maximal triiodothyronine-induced response) was measured for C, nonylphenol polyethoxylates and for D, cetyl alcohol polyethoxylates. Relative binding affinity to human TR $\beta$  was measured for E, nonylphenol polyethoxylates and F, cetyl alcohol polyethoxylates as percentage displacement of fluorescently labeled triiodothyronine from human TR $\beta$ . Coactivator recruitment of SRC2-2 to human TR $\beta$  was measured for the G, nonylphenol polyethoxylates and the H, cetyl alcohol polyethoxylates. Data presented as mean  $\pm$  SEM from 3 independent experiments. \*Lowest concentration with statistically significant effect; *P* less than .05, as per Kruskal-Wallis in GraphPad Prism 10. Dotted line represents half-maximal added agonist response for antagonism or binding affinity assays; decrease from baseline reflects antagonism of receptor and increase represents additive agonism response.

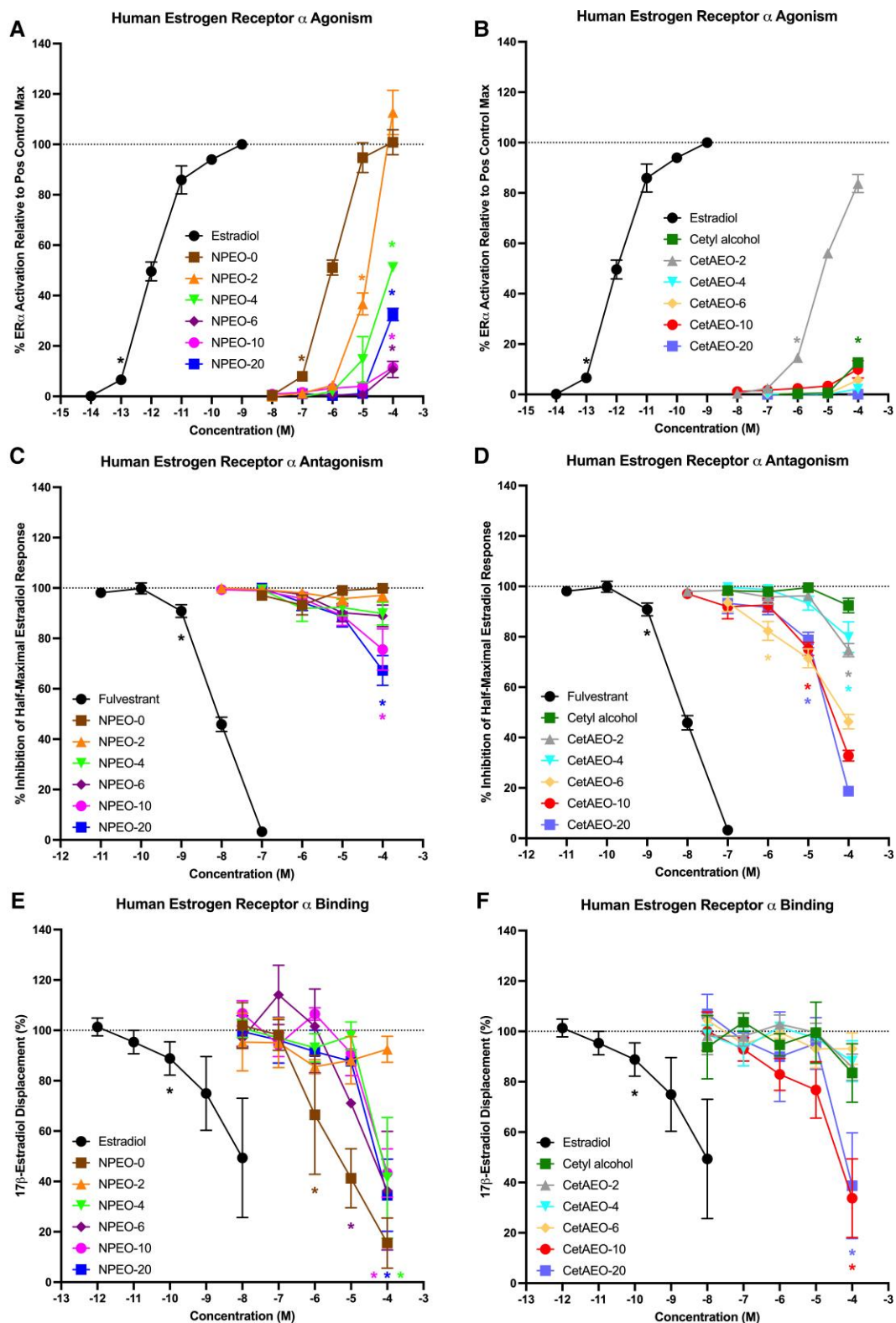


**Figure 7.** Estrogen receptor alpha (ER $\alpha$ ) bioactivities. Each polyethoxylate was tested for agonism, antagonism, and binding affinity for human ER $\alpha$ . Significant agonism of human ER $\alpha$  relative to the maximal 17 $\beta$ -estradiol response was measured for A, nonylphenol polyethoxylates and for B, cetyl alcohol polyethoxylates. Significant antagonism of human ER $\alpha$  (significant decrease in half-maximal estradiol-induced response) was measured for C, nonylphenol polyethoxylates and for D, cetyl alcohol polyethoxylates. Relative binding affinity to human ER $\alpha$  was measured for E, nonylphenol polyethoxylates and F, cetyl alcohol polyethoxylates as percentage displacement of fluorescently labeled estrone from human ER $\alpha$ . Data presented as mean  $\pm$  SEM from 3 independent experiments. \*Lowest concentration with statistically significant effect; *P* less than .05, as per Kruskal-Wallis in GraphPad Prism 10. Dotted line (A and B) represents mean positive control maximum response; may not always reflect exactly 100% due to differences in maximal concentration between assays. Dotted line (C-E) represents half-maximal added agonist response for antagonism or binding affinity assays; decrease from baseline reflects antagonism or displacement of agonist from receptor.

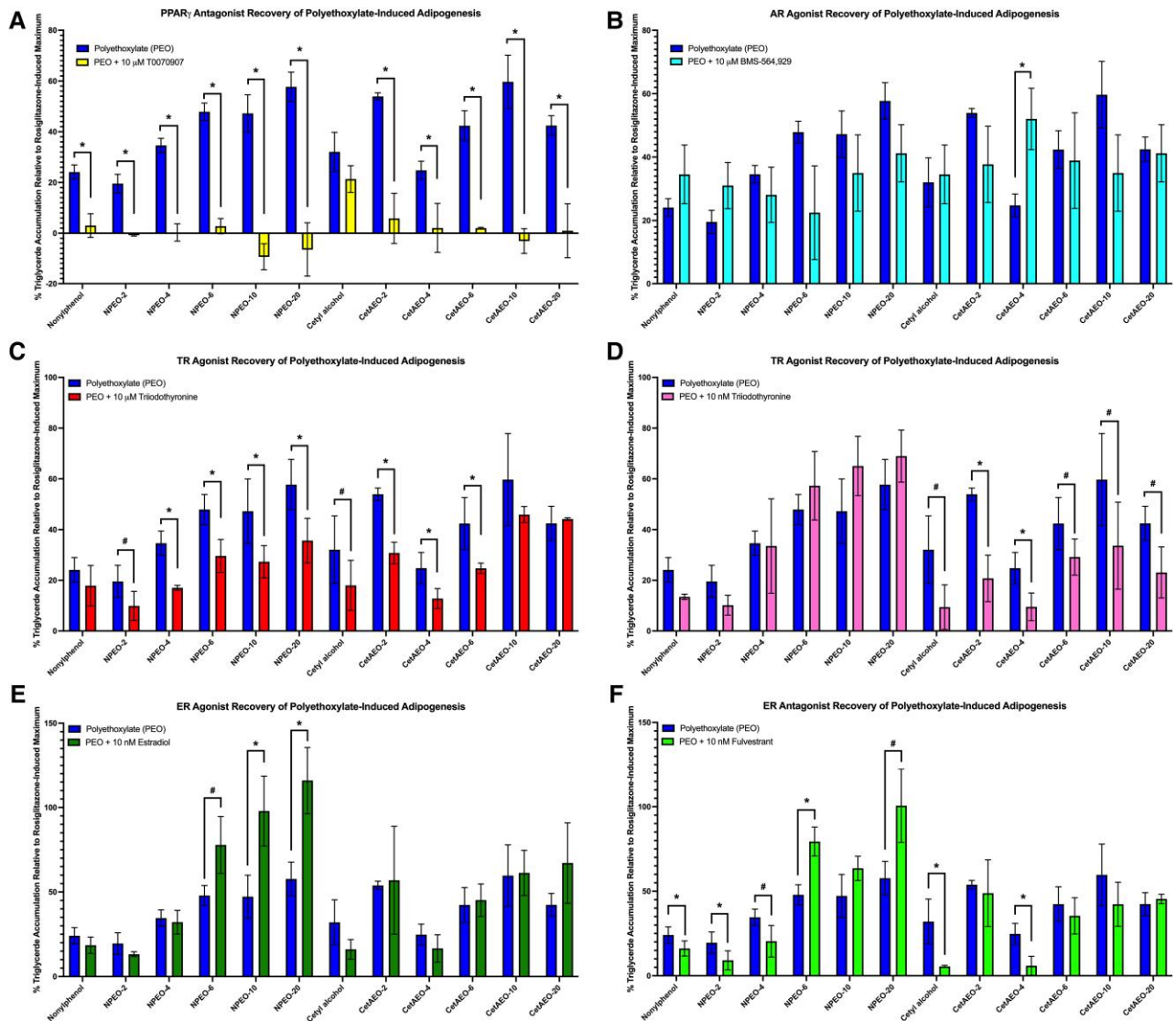


**Figure 8.** Human mesenchymal stem cells (hMSC) adipogenesis coexposure experiments. Each polyethoxylate was tested for triglyceride accumulation (marker for adipocyte differentiation) after 21 days of induction in hMSCs. Polyethoxylates were tested at 10  $\mu$ M concentrations and coexposures were performed with A, 10- $\mu$ M T0070907; B, 10- $\mu$ M BMS-564 929; C, 10- $\mu$ M triiodothyronine; D, 10-nM triiodothyronine; E, 10-nM 17 $\beta$ -estradiol; or F, 10-nM fulvestrant. Data presented as mean  $\pm$  SEM from 3 independent experiments. \*Statistically significant enhancement or attenuation of polyethoxylate-induced triglyceride accumulation; #P less than .05, as per Kruskal-Wallis in GraphPad Prism 10.

Zebrafish have 5 PPARs, including *pparaa*, *pparab*, *pparda*, *ppar db*, and *pparg* (69). Zebrafish PPAR $\gamma$  has 67% protein similarity to humans, with approximately 81% and 94%, respectively, of the ligand-binding domain and DNA-binding domain amino acids being identical (69). These differences, specifically the replacement of zebrafish PPAR $\gamma$  G312 and C313 by larger serine and tyrosine residues, have been reported to generate steric clashes that result in the inability of rosiglitazone to bind to and activate the receptor (69, 70). This has resulted in differing effects reported previously between zebrafish and human PPAR $\gamma$ , with rosiglitazone unable to activate zebrafish PPAR $\gamma$  in vitro (70-72). Interestingly, there are reports of metabolic health effects in zebrafish exposed to rosiglitazone (73) (though it specifically prevented the loss of adipose during a short-term starvation rather than promoting new adipose), suggesting differing responses in the whole organism model, nonspecific receptor-level effects, or effects via other signaling pathways such as the other zebrafish PPAR isoforms, which have not been as completely evaluated in

receptor activation as compared to human orthologues. This limited in vivo evidence also requires further substantiation.

PPAR $\gamma$  is generally considered the only nuclear receptor for which activation is necessary and sufficient to promote adipogenesis (74, 75), suggesting a likely causal role in adipogenic and/or obesogenic effects. Given this importance of PPAR $\gamma$  to adipogenesis, we tested for a causal/contributory role of PPAR $\gamma$  in the polyethoxylate-induced effects. Our coexposure experiments in hMSCs suggested a causal role for PPAR $\gamma$ , with PPAR $\gamma$  antagonist (T0070907) coexposure able to significantly decrease polyethoxylate-mediated triglyceride accumulation in the adipogenesis assay. However, given the critical importance of PPAR $\gamma$  to the adipogenic process, we then tested whether the inhibitory activity of T0070907 was specific to PPAR $\gamma$  or was nonspecific through coexposure testing with GR, TR, and AR ligands. The PPAR $\gamma$  antagonist robustly inhibited rosiglitazone-mediated adipogenesis but also nonspecifically inhibited adipogenesis promoted via flutamide, an AR antagonist, 1-850, a TR antagonist,

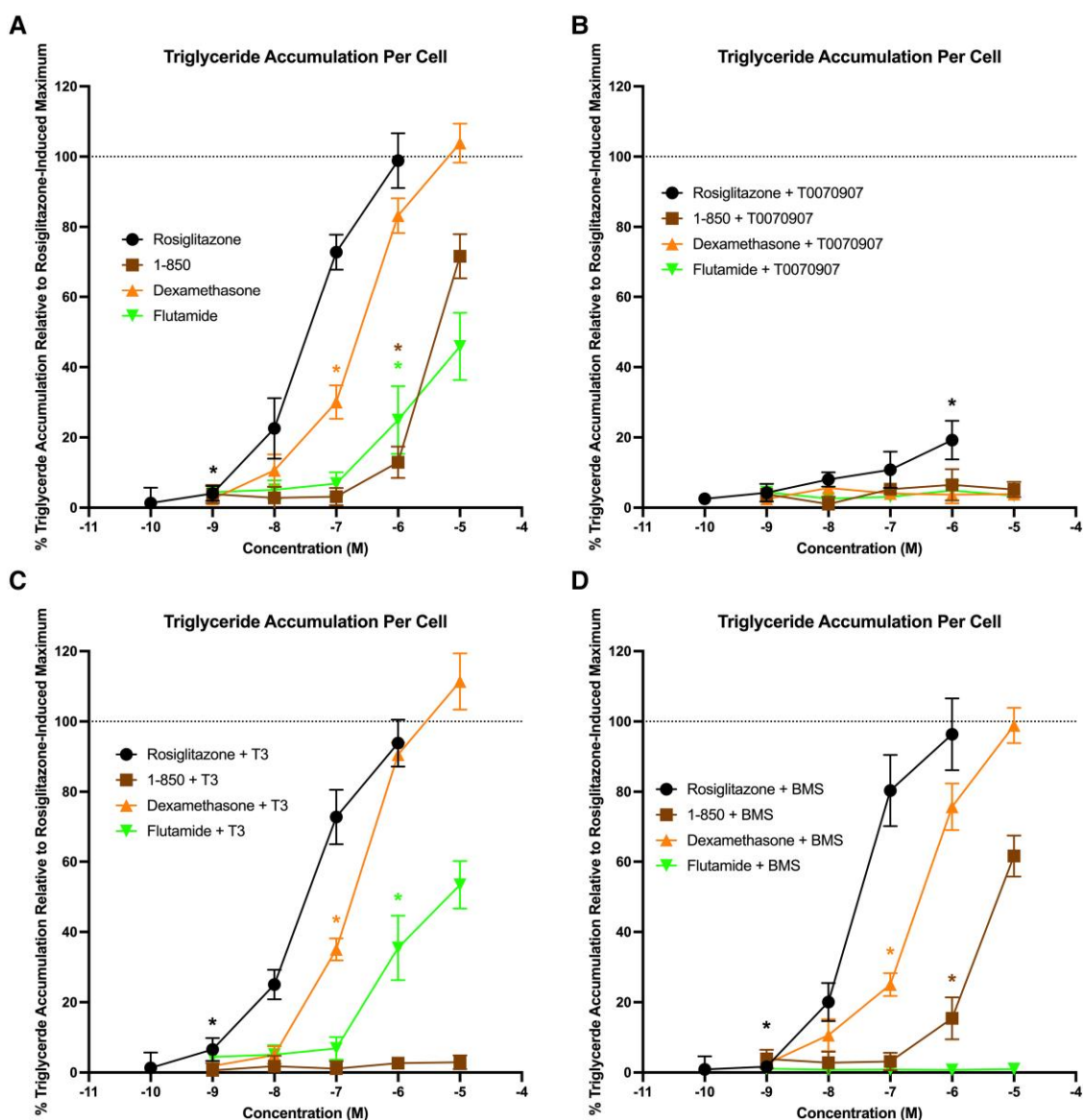


**Figure 9.** Specificity of control chemical adipogenic responses. Human mesenchymal stem cells were induced to differentiate as described in “Materials and Methods.” Cells were assessed for degree of adipocyte differentiation after 21 days of differentiation while exposed to control chemicals and coexposures. Triglyceride accumulation is provided as percentage of maximal rosiglitazone-induced triglyceride accumulation (maximal response when tested alone) and normalized to DNA content. Responses of these proadipogenic pathway ligands are examined A, alone; B, in combination with a set concentration of T0070907 (10  $\mu$ M); C, in combination with a set concentration of triiodothyronine (T3, 10  $\mu$ M), and D, in combination with a set concentration of BMS-564 929 (BMS, 10  $\mu$ M). Asterisks ( $P < .05$ ) denote the lowest concentration for each chemical with statistically significant differences from assay baseline responses, as per Kruskal-Wallis test.

and dexamethasone, a GR agonist. This suggests that the effect of T0070907 may not be PPAR $\gamma$  specific, though this cannot be determined precisely without further experiments. Previous data support a nonspecific inhibition of adipogenesis for T0070907, with no effects observed for the polyethoxylates on human PPAR $\gamma$  activation, binding, or coactivator recruitment (42). While there are thus clear and apparent species-specific differences across human and zebrafish receptors, these assays also used different positive control chemicals; rosiglitazone is the classic positive control for PPAR $\gamma$  but does not activate zebrafish PPAR $\gamma$  (70). Thus, comparability in the scale of response is more difficult due to differences in our respective control chemicals.

Based on similarities between effects on human and zebrafish receptors, AR and TR $\beta$  were then evaluated as potential causal pathways mediating the polyethoxylate-induced

adipogenic effects. The zebrafish AR is moderately well conserved (76), with 53% similarity to human AR overall, though 72% and 68% sequence similarity to human AR for the DNA and ligand binding domains, respectively (77). Moreover, some evidence suggests that antiandrogenic chemicals may act similarly between human and zebrafish ARs (78). In our study, the short-chain NPEOs (ie, nonylphenol, NPEO-2, NPEO-4) and CetAEO-4 exhibited greater AR antagonism for zebrafish AR than human AR, whereas the longer-chain length CetAEOs (ie, CetAEO-6, -10, and -20) exhibited greater human AR antagonism than for zebrafish AR. The longer-chain length NPEOs appeared to exhibit similar antagonism between the species, suggesting some molecular differences between these groups of polyethoxylates. Nonetheless, cotreatment with the AR agonist, BMS-564 929 did not

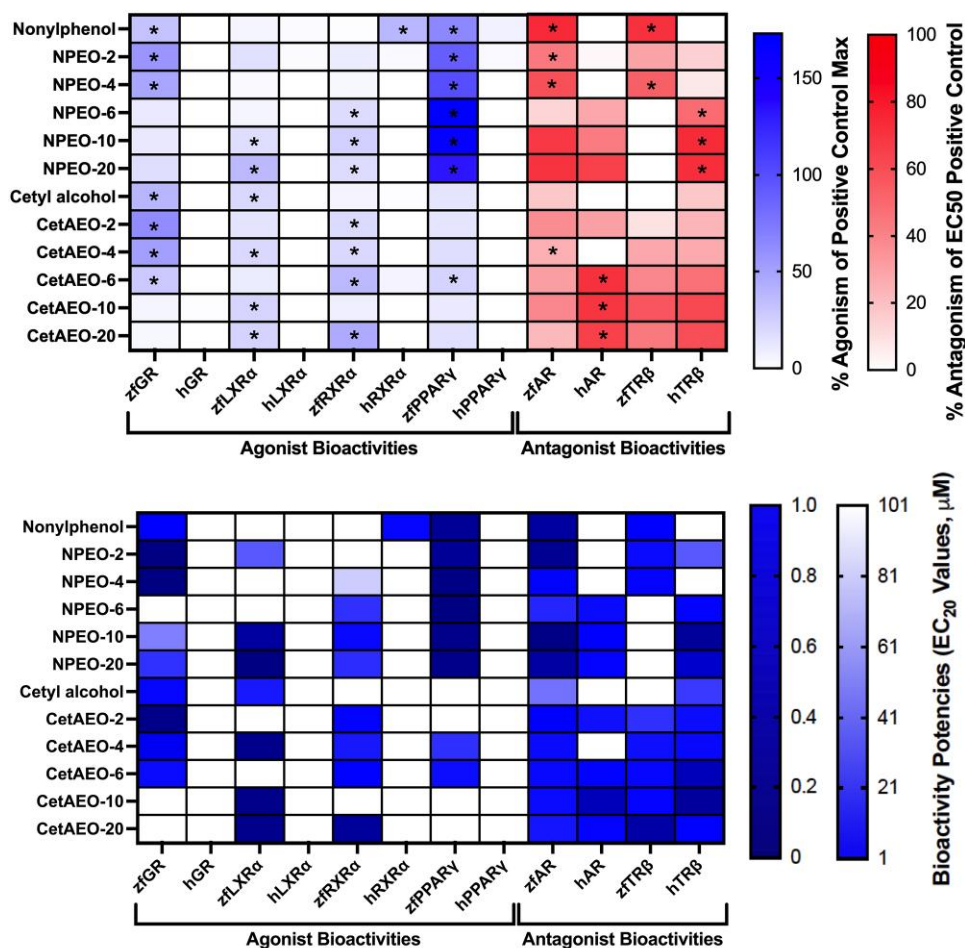


**Figure 10.** Receptor bioactivity species comparison. Heat map depicting the percentage maximal agonism or antagonism for each human and zebrafish receptor across the proadipogenic pathways evaluated here (top). Darker squares are higher efficacies for either agonism (to the left) or antagonism (to the right) of the figure. Heat map depicting the bioactivity potencies (EC<sub>20</sub> responses; concentrations at which 20% agonism or antagonism is observed) for each compound on each receptor (bottom). Darker squares are lower concentration potency values and represent higher potencies. \*Statistically significant differences between human and zebrafish maximal responses for that receptor bioactivity, with asterisk placed on the species with significantly greater activity. *P* less than .05, as per Kruskal-Wallis in GraphPad Prism 10.

meaningfully attenuate the polyethoxylate-induced triglyceride accumulation, suggesting that this is not a likely causal/contributory mechanism promoting the adipogenic effects *in vitro*.

Modulation of TR signaling is a robust proadipogenic pathway (53, 54, 64), and disruption of TR signaling is strongly associated with obesity (79, 80). TR action is important for the maintenance of metabolic health, lipid/carbohydrate metabolism, blood pressure regulation, and body mass homeostasis (81, 82). Hypothyroidism (decreased thyroid hormone) in humans is characterized by weight gain (79, 80) (hyperthyroidism is similarly characterized by weight loss), and hypothyroidism-induced weight gain can be reduced via therapeutic thyroid hormone supplementation (83-85). In line with this, antagonism of TR signaling promotes adipocyte differentiation *in vitro* (53, 86) and *in vivo* (87), though the mechanisms *in vitro* have not been sufficiently characterized. It is possible that the antagonism disrupts thyroid hormones normally present in the FBS of the differentiation media, though there is some evidence of reciprocal regulation of TRs and PPARs in adipogenesis (86).

There are 3 zebrafish TRs, including a genome duplication event for TR $\alpha$ , resulting in TR $\alpha$ A and TR $\alpha$ B as well as 2 TR $\beta$  isoforms (although the TR $\beta$  isoforms are identical other than a

9-amino acid insert in the hinge region between the ligand-binding domain and the DNA-binding domain) (88). There is high receptor conservation, with more than 80% sequence similarity for zebrafish TRs to human. Zebrafish TR $\alpha$ A and TR $\alpha$ B have 92% to 94% sequence similarity of the DNA-binding domain and 86% to 88% for the ligand-binding domain relative to human (88). There is even higher conservation for TR $\beta$ , with 86% overall sequence similarity, 92% for the DNA-binding domain, and 89% for the ligand-binding domain (88). Some limited previous research on TR $\beta$  binding comparisons specifically found equivalent binding affinities of T3 and thyroxine for human and zebrafish TR $\beta$ , though some species-specific differences for other environmental contaminants were observed (89). There is also some evidence that other thyroid hormones, such as 3,5-T2, are able to bind specifically to the TR $\beta$  isoform with the hinge region insert, but this does not appear to be the case for the canonical TR $\beta$  (90, 91) and thus we suspect this is not a contributory factor for our results. Specifically, halogenated bisphenols exhibited greater affinity for human TR $\beta$ , whereas halogenated phenols had greater affinity for zebrafish TR $\beta$  (89). This could explain the greater antagonism exhibited by the shorter-chain length NPEOs for zebrafish TR $\beta$ , given the phenolic ring, whereas the CetAEOs, without any phenolic

ring, had consistent responses between human and zebrafish TR $\beta$ . However, some of the longer-chain length polyethoxylates had greater antagonism for human TR $\beta$ , which requires further elucidation. Coexposure experiments supported a contributory role for TR antagonism in polyethoxylate-induced adipogenic effects, with high (10  $\mu$ M) T3 coexposure able to attenuate the triglyceride accumulation for all NPEOs, except for nonylphenol, as well as cetyl alcohol and CetAEOs-2 through -6. While this T3 coexposure was unable to modify the triglyceride accumulation induced by the longest-chain length CetAEOs, the lower (10 nM) T3 coexposure preferentially inhibited the triglyceride accumulation induced by the CetAEOs, including the longer-chain length CetAEOs, without any apparent effects on the NPEOs, suggesting that TR may play more of a contributory role for the CetAEOs than the NPEOs and effects at higher concentrations may be less specific. We additionally performed TR $\beta$  coactivator recruitment assays using SRC2-2 and demonstrated a putative agonistic effect both of NPEOs and CetAEOs recruiting SRC2-2, with much higher potency of effect observed for the CetAEOs, supporting a potential indirect mechanism of TR disruption that would support the relative binding affinity data and should be explored further.

Some limitations are inherent in our approach. We have yet to confirm these molecular mechanisms in zebrafish via coexposures and/or genetic modification experiments. Additionally, polyethoxylates were weakly active for zebrafish LXR, GR, and RXR, pathways where no appreciable human receptor activation was observed. While these pathways were not focused on due to the nonconcordance of effects between zebrafish and humans, future work should better delineate the mechanisms and implications of these differences. ER bioactivity determinations were performed only with the human receptor, and future work should involve acquisition and testing of zebrafish ER $\alpha$  for comparisons between the species isoforms. The longer-chain length CetAEOs expressed a high degree of human ER $\alpha$  antagonism, which was specific and direct, as per relative binding affinity assays, and could play a role in the adipogenic effects. However, coexposure experiments both with estradiol and fulvestrant had no statistically significant effects on these longer-chain length CetAEOs, suggesting they may not play a major contributory role in this activity. Interestingly, many of the NPEOs, which exhibited significant ER agonism, were inhibited with the fulvestrant coexposures; while the lower ER agonism, longer-chain length NPEOs exhibited enhanced triglyceride accumulation with the estradiol (E2) coexposures. While ER effects appeared to be direct, effects for TR $\beta$  appeared to be indirect, with the polyethoxylates unable to displace fluorescent T3 from the receptor, despite exhibiting robust receptor antagonism both in human and zebrafish reporter assays. This could occur through a number of mechanisms involving coregulatory protein recruitment, which we have begun to assess here and that demonstrate some effects of the polyethoxylates on coactivator recruitment to TR $\beta$ . Moreover, similar responses were observed for household dust samples, with T3 cotreatment attenuating dust sample-induced triglyceride accumulation in a similar adipogenesis model. House dust contains complex mixtures of NPEOs and CetAEOs (19), among other polyethoxylated surfactants, and small interfering RNA knockdown of TRs was also able to attenuate the dust-mediated effects (54), which should be reproduced with polyethoxylates specifically. This could provide further support for the TR $\beta$  antagonism reported previously in household dust

samples (92) and the causal role of that antagonism in adipogenic effects (54). We also observed relatively consistent inhibitions of triglyceride accumulation across the CetAEOs, regardless of extent of TR antagonism, though perhaps complicated by the differing effects on coactivator recruitment. Further research is needed to more conclusively examine this relationship. Interestingly, TR $\beta$  is not expressed in these cells in the basal state (precommitment and predifferentiation); this may suggest that the effects instead may be occurring through TR $\alpha$ , though nuclear receptor expression is reported to vary considerably throughout the commitment and differentiation processes (93). Further research should evaluate gene expression temporally to elucidate the specificity of these effects.

As discussed in greater detail earlier, metabolism of these polyethoxylates is well reported to occur through ethoxylate tail length shortening, which would produce the shorter chain length (and eventually base alkylphenol or alcohol) compounds. While more efficient tail length shortening has been reported with higher temperatures, potentially contributing to differing responses between human and zebrafish receptors, we would not expect this to vary between receptors. There is also the potential that shifts in temperature could influence octanol-water partition coefficient or other physicochemical parameters and could have influenced bioactivity independent of direct receptor modulation; binding experiments were performed at ambient temperature, zebrafish reporter bioassays at 28 °C, and human reporter bioassays at 37 °C. More direct assessments of receptor disruption and pharmacologic recovery can demonstrate direct effects and delineate how these pathways may differ between species. Lastly, there is a growing push for reducing and eliminating mammalian vertebrate animal use, which may contribute to greater reliance on alternate vertebrate models, such as zebrafish. Particularly in light of this, increased attention is needed to understand some of these interspecies' differences to ensure accurate translation to human health effects. It is important to note that consistent health effects were observed here, though some differences in mechanism were observed, suggesting that contaminants acting through these less-conserved mechanisms may have lower human health translation. Improving models of coculture and spheroids that may better reflect complex human physiology are important as regulators seek to transition away from murine models.

It is also important to place these results in perspective with environmental concentrations and presumed human exposures. Nonylphenol and its polyethoxylates tested here range in molecular weight from 220 to 1100 (cetyl alcohol polyethoxylates from 240-1120). Most of the examined bioactivities occurred at 1 and 10  $\mu$ M concentrations. This translates to parts per million (ppm) concentrations at 1  $\mu$ M of 0.24 to 2.4 ppm for cetyl alcohols and polyethoxylates and 1.12 to 11.2 ppm at 10  $\mu$ M. For nonylphenols and polyethoxylates, these concentrations are equivalent to 0.22 to 2.2 ppm at 1  $\mu$ M and 1.1 to 11 ppm at 10  $\mu$ M. These concentrations are regularly encountered in the environment, in surface, ground, and drinking water samples, and residential household dust (9, 36). While concentrations of alkylphenol and alcohol polyethoxylates generally occur in the 1 to 100s parts per billion range in natural waters and sediments (94-96), they are routinely found at low to moderate ppm concentrations in sediments and soils (97-104), in wastewater treatment plant and textile/paper mill effluents (105, 106), and near proximate contamination sources such as airports (107) or building materials (108). Further research is

needed to better delineate human exposure concentrations for these polyethoxylated compounds.

In conclusion, our research provides substantial insights into the molecular mechanisms underlying the adipogenic and obesogenic effects of NPEOs and CetAEOs both in human and zebrafish models. By employing paired receptor reporter gene assays, we identified substantial interspecies differences in receptor bioactivities, notably with PPAR $\gamma$ , RXR $\alpha$ , LXRA, and GR receptors. Zebrafish PPAR $\gamma$  exhibited robust agonism, suggesting species-specific interactions that may contribute to metabolism-disrupting effects, unlike human PPAR $\gamma$ , which showed no interaction with these polyethoxylates. The nonspecific inhibition of adipogenesis by the PPAR $\gamma$  antagonist, T0070907, indicates a potential broader mechanism of action beyond specific receptor pathways. Additionally, our findings highlight the differential responses of AR and TR $\beta$  pathways between human and zebrafish, with longer-chain polyethoxylates showing variable antagonistic effects. The attenuation of triglyceride accumulation through T3 coexposure underscores a contributory role for TR $\beta$  antagonism and/or broader thyroid hormone system disruption in the polyethoxylate-induced adipogenesis. While our study establishes a foundational understanding of these molecular interactions, further research is necessary to confirm these mechanisms in zebrafish models and explore additional pathways to fully elucidate the metabolic health effects of polyethoxylates. This work paves the way for future studies to better understand the environmental and health implications of these commonly encountered chemicals.

## Funding

This work was supported by the National Institute of Environmental Health Sciences (Nos. R00 ES030405 and P30 ES036084).

## Disclosures

The authors declare they have no actual or potential competing financial interests.

## Data Availability

Original data generated and analyzed during this study are included in this published article. Any further data in raw form is available on request.

## References

1. Marcomini A, Filipuzzi F, Giger W. Aromatic surfactants in laundry detergents and hard-surface cleaners: linear alkylbenzenesulphonates and alkylphenol polyethoxylates. *Chemosphere*. 1988;17(5):853-863.
2. Marcomini A, Stelluto S, Pavoni B. Determination of linear alkylbenzenesulphonates and alkylphenol polyethoxylates in commercial products and marine waters by reversed- and normal-phase HPLC. *Int J Environ Anal Chem*. 1989;35(4):207-218.
3. Maguire RJ. Review of the persistence of nonylphenol and nonylphenol ethoxylates in aquatic environments. *Water Qual Res J*. 1999;34(1):37-78.
4. Ying GG, Williams B, Kookana RS. Environmental fate of alkylphenols and alkylphenol ethoxylates—a review. *Environ Int*. 2002;28(3):215.
5. Loos R, Hanke G, Umlauf G, Eisenreich SJ. LC-MS-MS analysis and occurrence of octyl- and nonylphenol, their ethoxylates and their carboxylates in Belgian and Italian textile industry, waste water treatment plant effluents and surface waters. *Chemosphere*. 2007;66(4):690-699.
6. Bandiera SM. Reproductive and endocrine effects of p-nonylphenol and methoxychlor: a review. *Immunol Endocr Metab Agents Med Chem*. 2006;6(1):12.
7. Uguz C, Varisli O, Agca C, Agca Y. Effects of nonylphenol on motility and subcellular elements of epididymal rat sperm. *Reprod Toxicol*. 2009;28(4):542-549.
8. White R, Jobling S, Hoare SA, Sumpter JP, Parker MG. Environmentally persistent alkylphenolic compounds are estrogenic. *Endocrinology*. 1994;135(1):175-182.
9. Talmage SS. *Environmental and Human Safety of Major Surfactants: Alcohol Ethoxylates and Alkylphenol Ethoxylates*. The Soap and Detergent Association; 1994:374.
10. Marcomini A, Capri S, Giger W. Determination of linear alkylbenzenesulphonates, alkylphenol polyethoxylates and nonylphenol in waste water by high-performance liquid chromatography after enrichment on octadecylsilica. *J Chromatogr*. 1987;403:243-252.
11. Thurman EM, Ferrer I, Blotvogel J, et al. Analysis of hydraulic fracturing flowback and produced waters using accurate mass: identification of ethoxylated surfactants. *Anal Chem*. 2014;86(19):9653-9661.
12. Getzinger GJ, O'Connor MP, Hoelzer K, et al. Natural gas residual fluids: sources, endpoints, and organic chemical composition after centralized waste treatment in Pennsylvania. *Environ Sci Technol*. 2015;49(14):8347-8355.
13. Lester Y, Ferrer I, Thurman EM, et al. Characterization of hydraulic fracturing flowback water in Colorado: implications for water treatment. *Sci Total Environ*. 2015;512-513C:637-644.
14. Ahel M, Schaffner C, Giger W. Behaviour of alkylphenol polyethoxylate surfactants in the aquatic environment - III. Occurrence and elimination of their persistent metabolites during infiltration of river water to groundwater. *Water Res*. 1995;30(1):37-46.
15. Vega-Morales T, Sosa-Ferrera Z, Santana-Rodriguez JJ. Determination of alkylphenol polyethoxylates, bisphenol-A, 17 $\alpha$ -ethynylestradiol and 17 $\beta$ -estradiol and its metabolites in sewage samples by SPE and LC/MS/MS. *J Hazard Mater*. 2010;183(1-3):701-711.
16. Ferguson PL, Iden CR, Brownawell BJ. Analysis of alkylphenol ethoxylate metabolites in the aquatic environment using liquid chromatography—electrospray mass spectrometry. *Anal Chem*. 2000;72(18):4322-4330.
17. Ahel M, Giger W, Schaffner C. Behaviour of alkylphenol polyethoxylate surfactants in the aquatic environment - II. Occurrence and transformation in rivers. *Water Res*. 1994;28(5):1143-1152.
18. Clark LB, Rosen RT, Hartman TG, et al. Determination of alkylphenol ethoxylates and their acetic acid derivatives in drinking water by particle beam liquid chromatography/mass spectrometry. *Int J Environ Anal Chem*. 2006;47(3):167-180.
19. Ferguson, P.L., B. Vogler, and H.M. Stapleton. Non-targeted analysis to assess human exposure to semi-volatile organic contaminants in the indoor environment. In Proceedings of the 63rd ASMS Conference on Mass Spectrometry and Allied Topics. 2015. St. Louis, MO. [https://www.asms.org/docs/default-source/Past-Annual-Conference-Programs/asms-63rdprogram\\_www\\_v2.pdf](https://www.asms.org/docs/default-source/Past-Annual-Conference-Programs/asms-63rdprogram_www_v2.pdf)
20. Ferguson PL, Bopp RF, Chillrud SN, Aller RC, Brownawell B. Biogeochemistry of nonylphenol ethoxylates in urban estuarine sediments. *Environ Sci Technol*. 2003;37(16):3499-3506.
21. Giger W, Ahel M, Koch M, Laubscher HU, Schaffner C, Schneider J. Behaviour of alkylphenol polyethoxylate surfactants and of nitrilotriacetate in sewage treatment. *Water Sci Technol*. 1987;19(3-4):449-460.

22. Giger W, Brunner PH, Schaffner C. 4-nonylphenol in sewage sludge: accumulation of toxic metabolites from nonionic surfactants. *Science*. 1984;225(4662):623-625.
23. Ahel M, Giger W, Koch M. Behaviour of alkylphenol polyethoxylate surfactants in the aquatic environment - I. Occurrence and transformation in sewage treatment. *Water Res*. 1994;28(5):1131-1142.
24. Mann AH, Reid VW. Biodegradation of synthetic detergents evaluation by community trials part 2: alcohol and alkylphenol ethoxylates. *J Am Oil Chem Soc*. 1971;48(12):294-297.
25. Manzano MA, Perales JA, Sales D, Quiroga JM. The effect of temperature on the biodegradation of a nonylphenol polyethoxylate in river water. *Water Res*. 1999;33(11):2593-2600.
26. Newsted J, Tazelaar D, Kristofco L, Losey B. A meta-analysis of the occurrence of alkylphenols and alkylphenol ethoxylates in surface waters and sediments in the United States between 2010 and 2020. *Environ Pollut*. 2023;330:121757.
27. Agency, U.E.P. *Exposure Factors Handbook*. U.E.P. Agency, Editor; 2011.
28. Schmitz-Afonso I, Loyo-Rosales JE, de la Paz Avilés M, Rattner BA, Rice CP. Determination of alkylphenol and alkylphenolethoxylates in biota by liquid chromatography with detection by tandem mass spectrometry and fluorescence spectroscopy. *J Chromatogr A*. 2003;1010(1):25-35.
29. Cailleaud K, Forget-Leray J, Souissi S, Lardy S, Augagneur S, Budzinski H. Seasonal variation of hydrophobic organic contaminant concentrations in the water-column of the Seine Estuary and their transfer to a planktonic species *Eurytemora affinis* (Calanoid, copepod). Part 2: alkylphenol-polyethoxylates. *Chemosphere*. 2007;70(2):281-287.
30. Sabik H, Gagné F, Blaise C, Marcogliese DJ, Jeannot R. Occurrence of alkylphenol polyethoxylates in the St. Lawrence river and their bioconcentration by mussels (elliptio complanata). *Chemosphere*. 2003;51(5):349-356.
31. Dodder NG, Maruya KA, Lee Ferguson P, et al. Occurrence of contaminants of emerging concern in mussels (*Mytilus* spp.) along the California coast and the influence of land use, storm water discharge, and treated wastewater effluent. *Mar Pollut Bull*. 2014;81(2):340-346.
32. Lopez-Espinosa MJ, Freire C, Arrebola JP, et al. Nonylphenol and octylphenol in adipose tissue of women in southern Spain. *Chemosphere*. 2009;76(6):847-852.
33. Sise S, Uguz C. Nonylphenol in human breast milk in relation to sociodemographic variables, diet, obstetrics histories and lifestyle habits in a turkish population. *Iran J Public Health*. 2017;46(4):491-499.
34. Ringbeck B, Bury D, Hayen H, Weiss T, Brüning T, Koch HM. Determination of specific urinary nonylphenol metabolites by online-SPE-LC-MS/MS as novel human exposure biomarkers. *J Chromatogr B Analyt Technol Biomed Life Sci*. 2021;1177:122794.
35. Shin C, Lee SM, Kim M, Kim YS. Simultaneous determination of the free and total forms of nonylphenol, nonylphenol monoethoxylate, and nonylphenol diethoxylate in human urine by gas chromatography-mass spectrometry. *Anal Bioanal Chem*. 2023;415(26):6583-6593.
36. Babaei P, Nikravan Madan E, Güllü G, et al. Levels, distribution, sources and human exposure pathways of alkylphenol and alkylphenol ethoxylates in indoor dust in Turkiye. *Environ Pollut*. 2024;344:123447.
37. Jagani R, Chen J, Yelamanchili S, Wolff M, Andra S. Surfactant co-formulants in glyphosate-based herbicides: current gaps, and paths forward in human biomonitoring. *Chem Res Toxicol*. 2023;36(11):1653-1655.
38. Qiang S, Mohamed F, Mackenzie L, Roberts MS. Rapid determination of polyethoxylated tallow amine surfactants in human plasma by LC-MSMS. *Talanta*. 2023;254:124115.
39. Choyke S, Ferguson PL. Molecular characterization of nonionic surfactant components of the Corexit(R) 9500 oil spill dispersant by high-resolution mass spectrometry. *Rapid Commun Mass Spectrom*. 2019;33(22):1683-1694.
40. Herkert NJ, Kassotis CD, Zhang S, et al. Characterization of Per- and polyfluorinated alkyl substances present in commercial anti-fog products and their in vitro adipogenic activity. *Environ Sci Technol*. 2022;56(2):1162-1173.
41. Steeves KL, Bissram MJ, Kleywegt S, et al. Nontargeted screening reveals fluorotelomer ethoxylates in indoor dust and industrial wastewater. *Environ Int*. 2023;171:107634.
42. Kassotis CD, Kollitz EM, Ferguson PL, Stapleton HM. Nonionic ethoxylated surfactants induce adipogenesis in 3T3-L1 cells. *Toxicol Sci*. 2018;162(1):124-136.
43. Kassotis CD, LeFauve MK, Chiang YT, Knuth MM, Schkoda S, Kullman SW. Nonylphenol polyethoxylates enhance adipose deposition in developmentally exposed zebrafish. *Toxics*. 2022;10(2):99.
44. LeFauve MK, Bérubé R, Heldman S, Chiang YT, Kassotis CD. Cetyl alcohol polyethoxylates disrupt metabolic health in developmentally exposed zebrafish. *Metabolites*. 2023;13(3):359.
45. Sanderson H, van Compernelle R, Dyer SD, et al. Occurrence and risk screening of alcohol ethoxylate surfactants in three U.S. River sediments associated with wastewater treatment plants. *Sci Total Environ*. 2013;463-464:600-610.
46. Life Technologies. LanthaScreen™ TR-FRET Thyroid Receptor Beta Coactivator Assay. 2014. Accessed November 1, 2024. [https://assets.thermofisher.com/TFSAssets/LSG/manuals/lanthascreen\\_TR\\_beta\\_man.pdf](https://assets.thermofisher.com/TFSAssets/LSG/manuals/lanthascreen_TR_beta_man.pdf)
47. Cheng S, Eberhardt NL, Robbins J, Baxter JD, Pastan I. Fluorescent rhodamine-labeled thyroid hormone derivatives: synthesis and binding to the thyroid hormone nuclear receptor. *FEBS Lett*. 1979;100(1):113-116.
48. Taylor E, Heyland A. Thyroid hormones accelerate initiation of skeletogenesis via MAPK (ERK1/2) in Larval Sea Urchins (strongylocentrotus purpuratus). *Front Endocrinol (Lausanne)*. 2018;9:439.
49. Technologies L. *PolarScreen Nuclear Receptor Competitor Assays*. Universal Protocol; 2014.
50. Invitrogen. LanthaScreen™ TR-FRET Thyroid Receptor beta Coactivator Assay. 2007. Accessed November 1, 2024. [https://assets.thermofisher.com/TFS-Assets/LSG/manuals/lanthascreen\\_TR\\_beta\\_man.pdf](https://assets.thermofisher.com/TFS-Assets/LSG/manuals/lanthascreen_TR_beta_man.pdf)
51. Bérubé R, LeFauve MK, Heldman S, et al. Adipogenic and endocrine disrupting mixture effects of organic and inorganic pollutant mixtures. *Sci Total Environ*. 2023;876:162587. In press.
52. Chiang YT, Kassotis CD. Molecular assessment of pro-adipogenic effects for common-use contraceptives and their mixtures. *Endocrinology*. 2024;165(6):bqae050. In press.
53. Kassotis CD, Masse L, Kim S, Schlezinger JJ, Webster TF, Stapleton HM. Characterization of adipogenic chemicals in three different cell culture systems: implications for reproducibility based on cell source and handling. *Sci Rep*. 2017;7(1):42104.
54. Kassotis CD, Kollitz EM, Hoffman K, Sosa JA, Stapleton HM. Thyroid receptor antagonism as a contributory mechanism for adipogenesis induced by environmental mixtures in 3T3-L1 cells. *Sci Total Environ*. 2019;666:431-444.
55. Kassotis CD, Hoffman K, Phillips AL, et al. Characterization of adipogenic, PPARgamma, and TRbeta activities in house dust extracts and their associations with organic contaminants. *Sci Total Environ*. 2020;758:143707.
56. Kassotis CD, Hoffman K, Völker J, et al. Reproducibility of adipogenic responses to metabolism disrupting chemicals in the 3T3-L1 pre-adipocyte model system: an interlaboratory study. *Toxicology*. 2021;461:152900.
57. Filer D, Hoffman K, Sargis RM, Trasande L, Kassotis CD. On the utility of ToxCast-based predictive models to evaluate potential metabolic disruption by environmental chemicals. *Environ Health Perspect*. 2022;130(5):57005.
58. Andrews S. FastQC: A Quality Control Tool for High Throughput Sequence Data. 2010. Accessed November 1, 2024. <https://www.bioinformatics.babraham.ac.uk/projects/fastqc/>

59. Dobin A, Davis CA, Schlesinger F, *et al.* STAR: ultrafast universal RNA-seq aligner. *Bioinformatics*. 2013;29(1):15-21.
60. Anders S, Pyl PT, Huber W. HTSeq—a python framework to work with high-throughput sequencing data. *Bioinformatics*. 2015;31(2):166-169.
61. Robinson MD, McCarthy DJ, Smyth GK. Edger: a bioconductor package for differential expression analysis of digital gene expression data. *Bioinformatics*. 2010;26(1):139-140.
62. Huang da W, Sherman BT, Lempicki RA. Systematic and integrative analysis of large gene lists using DAVID bioinformatics resources. *Nat Protoc*. 2009;4(1):44-57.
63. Edgar R, Domrachev M, Lash AE. Gene expression omnibus: NCBI gene expression and hybridization array data repository. *Nucleic Acids Res*. 2002;30(1):207-210.
64. Kassotis CD, Stapleton HM. Endocrine-mediated mechanisms of metabolic disruption and new approaches to examine the public health threat. *Front Endocrinol (Lausanne)*. 2019;10:39.
65. Kassotis CD, Vom Saal FS, Babin PJ, *et al.* Obesity III: obesogen assays: limitations, strengths, and new directions. *Biochem Pharmacol*. 2022;199:115014.
66. Jobling S, Sumpter JP. Detergent components in sewage effluent are weakly oestrogenic to fish: an in vitro study using rainbow trout (*oncorhynchus mykiss*) hepatocytes. *Aquat Toxicol*. 1993;27(3-4):361-372.
67. Heindel JJ, Howard S, Agay-Shay K, *et al.* Obesity II: establishing causal links between chemical exposures and obesity. *Biochem Pharmacol*. 2022;199:115015.
68. Lustig RH, Collier D, Kassotis C, *et al.* Obesity I: overview and molecular and biochemical mechanisms. *Biochem Pharmacol*. 2022;199:115012.
69. Den Broeder MJ, Kopylova VA, Kamminga LM, Legler J. Zebrafish as a model to study the role of peroxisome proliferating-activated receptors in adipogenesis and obesity. *PPAR Res*. 2015;2015:358029.
70. Garoche C, Boulahouf A, Grimaldi M, *et al.* Interspecies differences in activation of peroxisome proliferator-activated receptor gamma by pharmaceutical and environmental chemicals. *Environ Sci Technol*. 2021;55(24):16489-16501.
71. Riu A, McCollum CW, Pinto CL, *et al.* Halogenated bisphenol-A analogs act as obesogens in zebrafish larvae (*Danio rerio*). *Toxicol Sci*. 2014;139(1):48-58.
72. Riu A, Grimaldi M, le Maire A, *et al.* Peroxisome proliferator-activated receptor gamma is a target for halogenated analogs of bisphenol A. *Environ Health Perspect*. 2011;119(9):1227-1232.
73. Tingaud-Sequeira A, Ouadah N, Babin PJ. Zebrafish obesogenic test: a tool for screening molecules that target adiposity. *J Lipid Res*. 2011;52(9):1765-1772.
74. Rosen ED, Sarraf P, Troy AE, *et al.* PPAR gamma is required for the differentiation of adipose tissue in vivo and in vitro. *Mol Cell*. 1999;4(4):611-617.
75. Rosen ED, Spiegelman BM. Molecular regulation of adipogenesis. *Annu Rev Cell Dev Biol*. 2000;16(1):145-171.
76. Hossain MS, Larsson A, Scherbak N, Olsson PE, Orban L. Zebrafish androgen receptor: isolation, molecular, and biochemical characterization. *Biol Reprod*. 2008;78(2):361-369.
77. Gorelick DA, Watson W, Halpern ME. Androgen receptor gene expression in the developing and adult zebrafish brain. *Dev Dyn*. 2008;237(10):2987-2995.
78. Smolinsky AN, Doughman JM, Kratzke LT, Lassiter CS. Zebrafish (*Danio rerio*) androgen receptor: sequence homology and up-regulation by the fungicide vinclozolin. *Comp Biochem Physiol C Toxicol Pharmacol*. 2010;151(2):161-166.
79. Kolyvanos Naumann K, Furer J, Käser L, Vetter W. [Hypothyroidism. Main symptoms: fatigue, weight gain, depression, myalgia, edema]. *Praxis (Bern 1994)*. 2007;96(38):1411-1417. quiz 1418-9.
80. Bratusch-Marrain P, Schmid P, Waldhäusl W, Schlick W. Specific weight loss in hyperthyroidism. *Horm Metab Res*. 1978;10(5):412-415.
81. Obregon MJ. Thyroid hormone and adipocyte differentiation. *Thyroid*. 2008;18(2):185-195.
82. Shulman AI, Mangelsdorf DJ. Retinoid x receptor heterodimers in the metabolic syndrome. *N Engl J Med*. 2005;353(6):604-615.
83. Bryzgalova G, Effendic S, Khan A, *et al.* Anti-obesity, anti-diabetic, and lipid lowering effects of the thyroid receptor beta subtype selective agonist KB-141. *J Steroid Biochem Mol Biol*. 2008;111(3-5):262-267.
84. Dale J, Daykin J, Holder R, *et al.* Weight gain following treatment of hyperthyroidism. *Clin Endocrinol (Oxf)*. 2001;55(2):233-239.
85. Lonn L, Stenlöf K, Ottosson M, Lindroos AK, Nyström E, Sjöström L. Body weight and body composition changes after treatment of hyperthyroidism. *J Clin Endocrinol Metab*. 1998;83(12):4269-4273.
86. Lu C, Cheng SY. Thyroid hormone receptors regulate adipogenesis and carcinogenesis via crosstalk signaling with peroxisome proliferator-activated receptors. *J Mol Endocrinol*. 2010;44(3):143-154.
87. Kindblom JM, Gevers EF, Skrtic SM, *et al.* Increased adipogenesis in bone marrow but decreased bone mineral density in mice devoid of thyroid hormone receptors. *Bone*. 2005;36(4):607-616.
88. Darras VM, Van Herck SL, Heijlen M, De Groef B. Thyroid hormone receptors in two model species for vertebrate embryonic development: chicken and zebrafish. *J Thyroid Res*. 2011;2011:402320.
89. Kollitz EM, De Carbonnel L, Stapleton HM, Lee Ferguson P. The affinity of brominated phenolic compounds for human and zebrafish thyroid receptor beta: influence of chemical structure. *Toxicol Sci*. 2018;163(1):226-239.
90. Mendoza A, Navarrete-Ramírez P, Hernández-Puga G, *et al.* 3,5-T2 is an alternative ligand for the thyroid hormone receptor beta1. *Endocrinology*. 2013;154(8):2948-2958.
91. Lazcano I, Rodríguez-Ortiz R, Villalobos P, Martínez-Torres A, Solís-Sainz JC, Orozco A. Knock-down of specific thyroid hormone receptor isoforms impairs body plan development in zebrafish. *Front Endocrinol (Lausanne)*. 2019;10:156.
92. Kollitz EM, Kassotis CD, Hoffman K, Ferguson PL, Sosa JA, Stapleton HM. Chemical mixtures isolated from house dust disrupt thyroid receptor  $\beta$  (TR $\beta$ ) signaling. *Environ Sci Technol*. 2018;52(20):11857-11864.
93. Fu M, Sun T, Bookout AL, *et al.* A nuclear receptor atlas: 3T3-L1 adipogenesis. *Mol Endocrinol*. 2005;19(10):2437-2450.
94. Klosterhaus S, Allen R, Davis JA. *Contaminants of Emerging Concern in the San Francisco Estuary: Alkylphenol Ethoxylates*. SFEI Contribution No. 657. SFEI; 2012:17. [https://www.sfei.org/sites/default/files/biblio\\_files/Alkylphenol\\_Ethoxylates\\_profile\\_finalv2\\_0.pdf](https://www.sfei.org/sites/default/files/biblio_files/Alkylphenol_Ethoxylates_profile_finalv2_0.pdf)
95. Lindborg A, Overdahl KE, Vogler B, Lin D, Sutton R, Ferguson PL. *Assessment of Long-Chain Polyethoxylate Surfactants in Wastewater Effluent, Stormwater Runoff, and Ambient Water of San Francisco Bay, CA*. ACS ES&T Water, 2023. 3(4).
96. DiLoreto S. *Analysis of Ethoxylated Surfactants and Their Degradation Products in Ambient Water, Wastewater, and Stormwater of San Francisco Bay, CA, in Nicholas School of the Environment*. Duke University; 2023:28.
97. Jardak K, Drogui P, Daghrir R. Surfactants in aquatic and terrestrial environment: occurrence, behavior, and treatment processes. *Environ Sci Pollut Res Int*. 2016;23(4):3195-3216.
98. Ying GG, Williams B, Kookana R. Environmental fate of alkylphenols and alkylphenol ethoxylates—a review. *Environ Int*. 2002;28(3):215-226.
99. Marcomini A, Pavoni B, Sfriso A, *et al.* Persistent metabolites of alkylphenol polyethoxylates in the marine environment. *Mar Chem*. 1990;29:307-323.
100. Bennie DT, Sullivan CA, Lee HB, Maguire RJ. Alkylphenol polyethoxylate metabolites in Canadian sewage treatment plant waste streams. *Water Qual Res J*. 1998;33(2):231-252.
101. Ferguson PL, Iden CR, Brownawell BJ. Distribution and fate of neutral alkylphenol ethoxylate metabolites in a sewage-

- impacted urban estuary. *Environ Sci Technol.* 2001;35(12):2428-2435.
102. Mahalakshmi R, Pugazhendhi A, Brindhadevi K, Ramesh N. Analysis of alkylphenol ethoxylates (APEOs) from tannery sediments using LC-MS and their environmental risks. *Process Biochem.* 2020;97:37-42.
103. Shiu R-F, Jiang J-J, Kao H-Y, *et al.* Alkylphenol ethoxylate metabolites in coastal sediments off southwestern Taiwan: spatiotemporal variations, possible sources, and ecological risk. *Chemosphere.* 2019;225:9-18.
104. Klancic V, Gobec M, Jakopin Z. Environmental contamination status with common ingredients of household and personal care products exhibiting endocrine-disrupting potential. *Environ Sci Pollut Res Int.* 2022;29(49):73648-73674.
105. Bennie DT. Review of the environmental occurrence of alkylphenols and alkylphenol ethoxylates. *Water Qual Res J.* 1999;34(1):79-122.
106. Hale RC, Smith CL, de Fur PO, *et al.* Nonylphenols in sediments and effluents associated with diverse wastewater outfalls. *Environ Toxicol Chem.* 2009;19(4):946-952.
107. Corsi SR, Zitomer DH, Field JA, Cancilla DA. Nonylphenol ethoxylates and other additives in aircraft deicers, anticlers, and waters receiving airport runoff. *Environ Sci Technol.* 2003;37(18):4031-4037.
108. Janousek RM, Muller J, Knepper TP. Combined study of source, environmental monitoring and fate of branched alkylphenols: the chain length matters. *Chemosphere.* 2020;241:124950.